

Materials characterization at the nanoscale by X-ray spectrometry

Burkhard Beckhoff

Physikalisch-Technische Bundesanstalt
Abbestraße 2-12, 10587 Berlin, Germany

- **analytical challenges for nanotechnologies**
- **reference-free x-ray spectrometry**
- **surface contamination and nanolayer characterization**
- **depth profiling at grazing incidence**
- **chemical speciation at buried interfaces**
- **towards in-situ speciation of bulk-type films**
- **high-resolution spectrometry**

Analytical challenges for nanotechnologies

- dozens of **new nanoscaled materials** appear every month
- **technology R&D cycles** for new materials down to 4 months
- **need for correlation** of material properties with functionality
- **requirements** on sensitivity, selectivity and information depth
- most **analytical methodologies** rely on **reference materials** or calibration standards but there are only few at the nanoscale
- usage of **calibrated instrumentation** and knowledge on atomic data enables **reference-free techniques** such as SR based XRS

Challenges for nanotechnologies – nano-scaled reference materials

Nanoscaled Reference Materials (in line with ISO/TC 229 Nanotechnologies)

Reference materials are the key to guaranteeing reliability and correctness for results of chemical analyses and technical measurements.'

Categories:

- flatness
- film thickness
- single step , periodic step, step grating
- lateral X-Y-axis, 1-dim
- lateral X-Y-axis, +2-dim,
- critical dimensions
- 3-dimensional
- nanoobjects/nanoparticles/nanomaterial
- nanocrystallite materials
- porosity
- depth profiling resolution

Every month several tens new nanoscaled materials appear.

The number of nanoscaled reference materials is considerably lower.

Reference-free / first principles based methodologies can address this increasing gap.

Challenges for nanotechnologies – nano-scaled reference materials

Nanoscaled Reference Materials (in line with ISO/TC 229 Nanotechnologies)

Reference materials are the key to guaranteeing reliability and correctness for results of chemical analyses and technical measurements. ‘

Categories:

- flatness
- **film thickness**
- single step , periodic step, step grating
- lateral X-Y-axis, 1-dim
- lateral X-Y-axis, +2-dim,
- critical dimensions
- 3-dimensional
- **nanoobjects/nanoparticles/nanomaterial**
- nanocrystallite materials
- porosity
- **depth profiling resolution**

| Description | Certified values (nm) | RM name | RM type | RM no. |
|---|--------------------------------|-----------------|---------|--------|
| Ti-Al multilayer 100/250 nm on 100Cr6 steel substrate | 100 | BAM L-100 | CRM | 12 |
| Thickness standards, tantalum pentoxide film Calibration of depth-resolving surface analysis | 30 | BCR-261 | CRM | 13 |
| Thickness standard, silicon dioxide film NIST traceable | (2, 4.5, 7.5, 12, 25, 50, ...) | FTS | RM | 3 |
| Thickness standards, silicon nitride film NIST traceable | 20 | NFTS | RM | 10 |
| Thickness standards, tungsten film For best performance with sonar technology, an oxide layer 100 nm thick is added between the silicon substrate and the metal film, traceable to NIST | 200 | WFTS | RM | 11 |
| GaAs/AlAs-superlattice Calibration of depth resolution | 23 | CRM 5201-a | CRM | 32 |
| SiO2/Si multilayer film reference material Consist of five layers with SiO2 and Sigrown using r.f. magnetron sputtering method on aSi substrate. The thickness of each layer is certified in units of length via X-ray reflectometry, control the precision of analysis and to regulate measurement condition in depth profile analysis by ion | 20 | NMIJ CRM 5202-a | CRM | 54 |
| GaAs/AlAs super lattice The CRM has six-layer-structure and the certified values for the thickness from the second to sixth layer are given; control the precision of analysis and to regulate measurement condition in depth profile analysis by ion sputtering | 9,51 | NMIJ CRM 5203-a | CRM | 55 |
| Ultrathin silicon dioxide film 3.49 nm (0.19 nm); control the precision of analysis and to regulate measurement condition in depth profile analysis by ion sputtering | 3,49 | NMIJ CRM 5204-a | CRM | 56 |

Synchrotron radiation based x-ray spectrometry

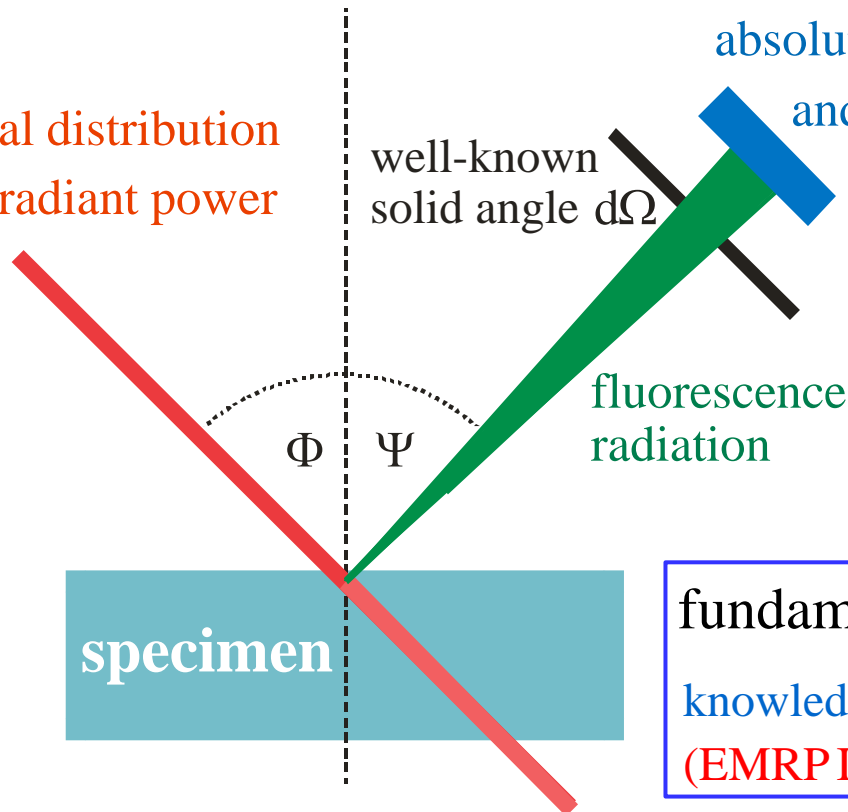
XRS excitation channel:

well-known spectral distribution
and a well-known radiant power

XRS detection channel:

absolute detection efficiency
and response functions

derived from
x-ray radiometry



specimen

fluorescence
radiation

well-known
solid angle $d\Omega$

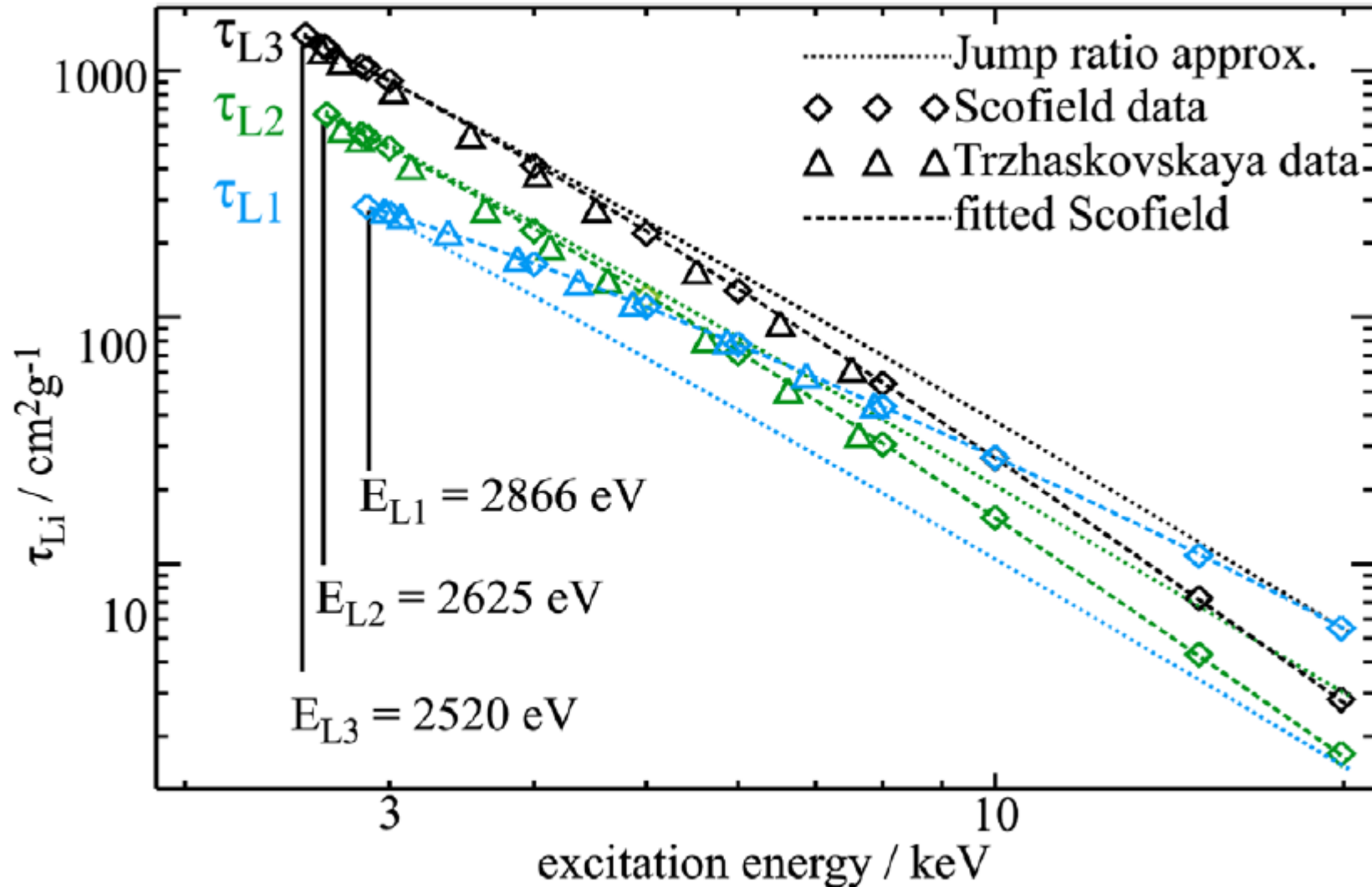
fundamental parameters
knowledge of atomic parameters
(EMRP IND07, NEW01, ENG53)

PTB capabilities:

- characterized beamlines
- calibrated photodiodes
- calibrated diaphragms
- calibrated Si(Li) detectors

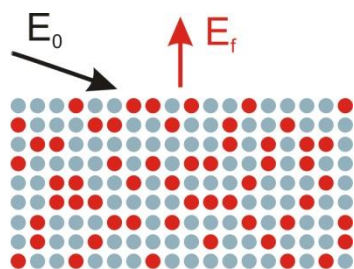
transmission measurements
absorption correction factors

Determination of L-shell photoionization cross sections



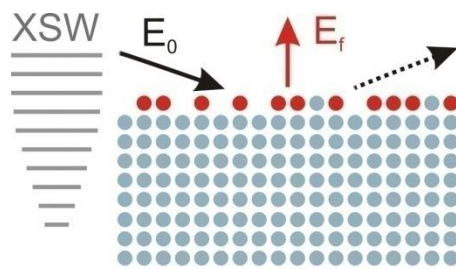
Tuning the analytical sensitivity and information depth by means of appropriate operational parameters

excitation conditions



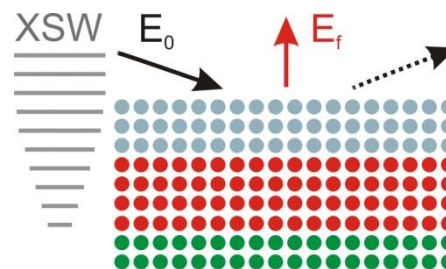
concentration

total-reflection



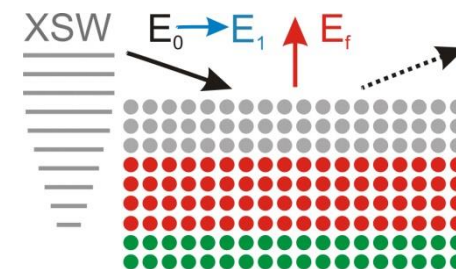
contamination

tunable incident angle



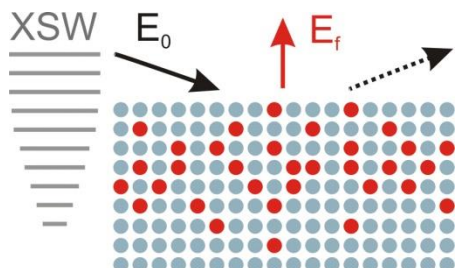
nanolayer

tunable photon energy



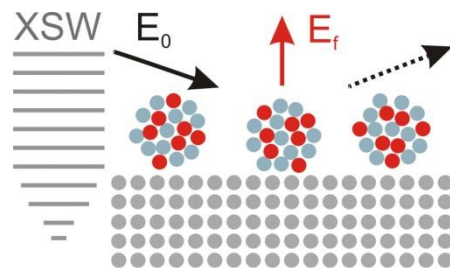
nanolayer speciation

tunable incident angle



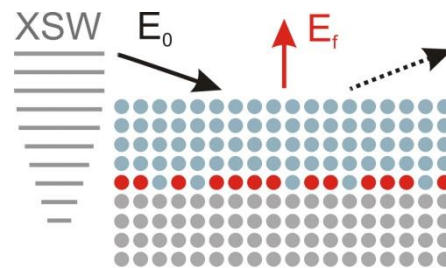
depth profile

total-reflection



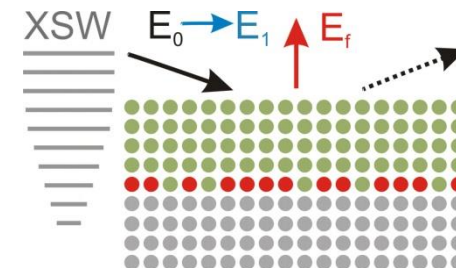
nanoparticles

tunable incident angle



interface

tunable photon energy



interface speciation

E_0 = photon energy of excitation radiation

E_1 = photon energy above absorption edge

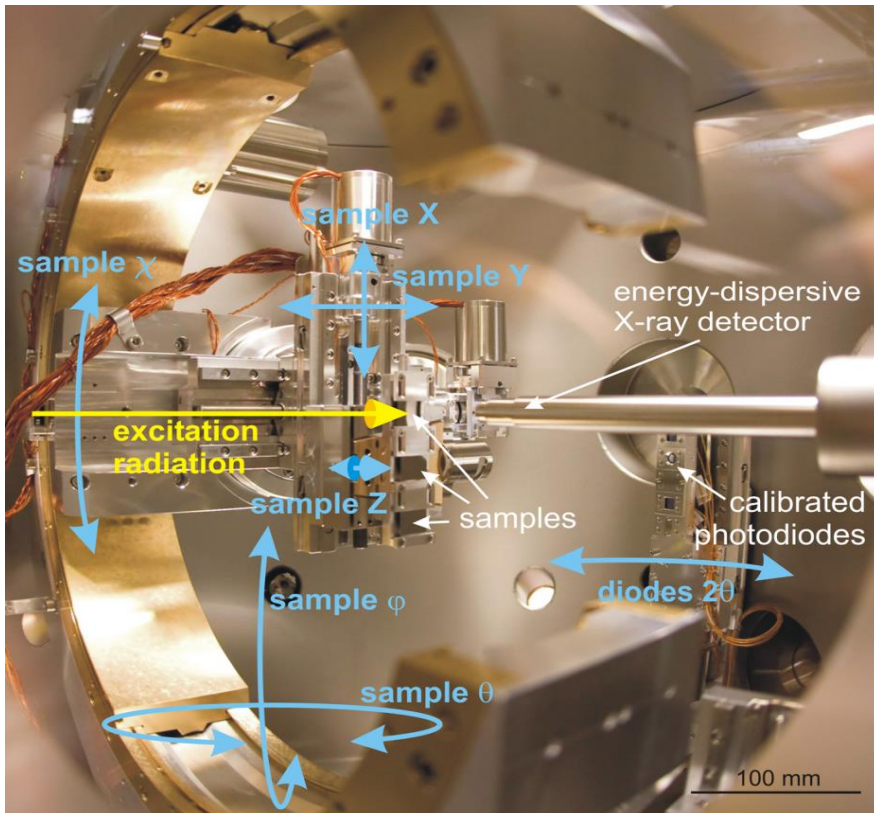
E_f = photon energy of fluorescence radiation

XSW = X-ray Standing Wave field

J. Anal. At. Spectrom. **23**, 845 (2008)

Novel XRS instrumentation for advanced materials characterizations with synchrotron radiation

PTB XRS instrumentation at BESSY

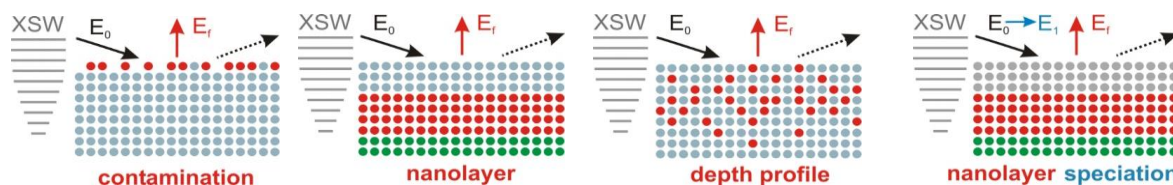


9-axis manipulator and chamber ensuring

- the entire TXRF, GIXRF and XRF regime
- polarization-dependent speciation by XAFS
- combined GIXRF and XRR investigations
- movable aperture system for reference-free XRF and atomic FP determinations

Transfer of modified instrumentation to

- TU Berlin for a **laboratory plasma source**
- LNE/CEA-LNHB for **SOLEIL storage ring**
- IAEA (UN) for **ELETTRA storage ring**



Janin Lubeck et al.,

Rev. Sci. Instrum. **84**, 045106 (2013)

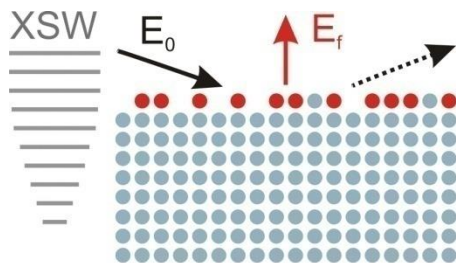
Quantitation in SR-TXRF routine analysis on Si wafers

TXRF spectra deconvolution

including Si(Li) detector response functions, RRS, and bremsstrahlung contributions.

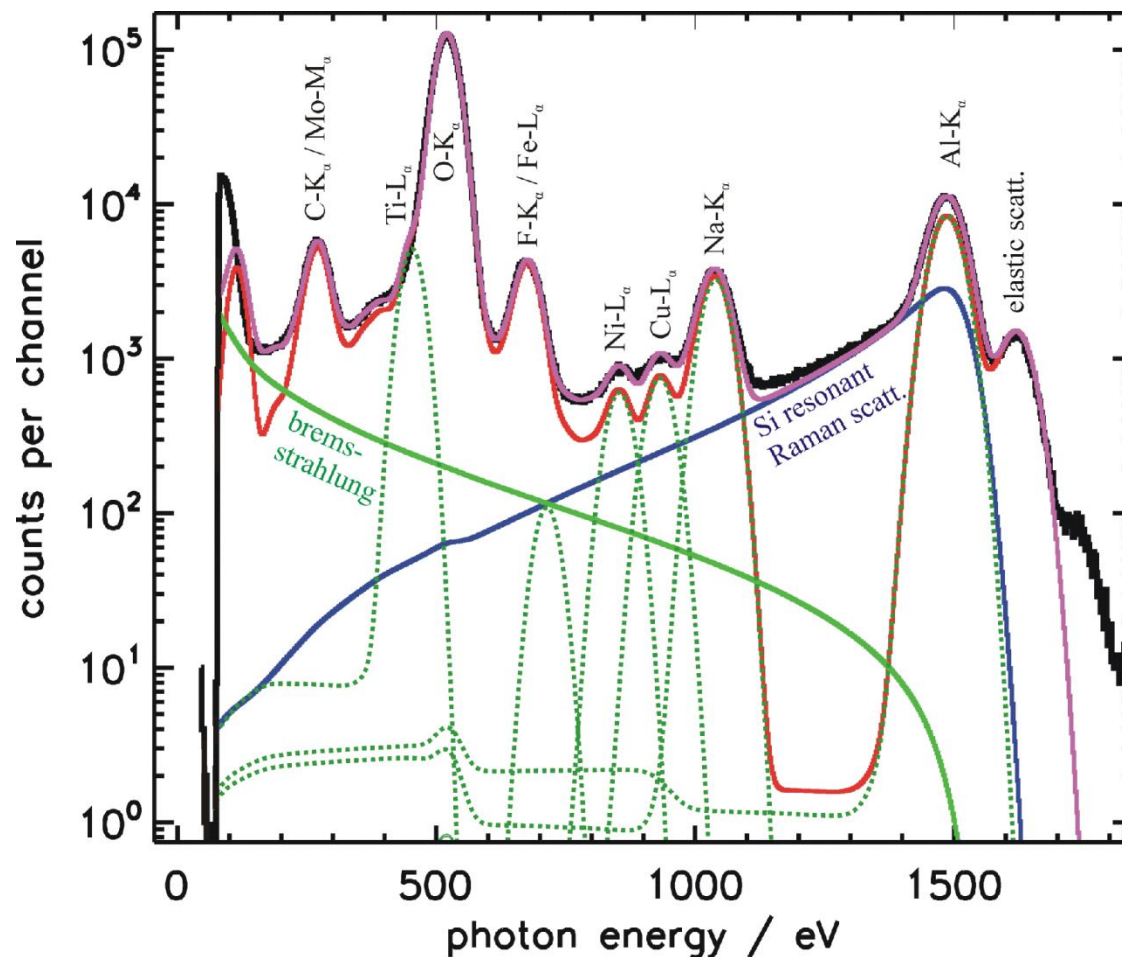
reference-free TXRF

quantitation: known incident flux, detector efficiency and solid angle.



contamination

spin-coated wafer with 10^{12} cm^{-2} of various transition metals



Reference-free quantitation in SR-TXRF analysis

mass deposition m_i / F_I of the element i with unit area F_I

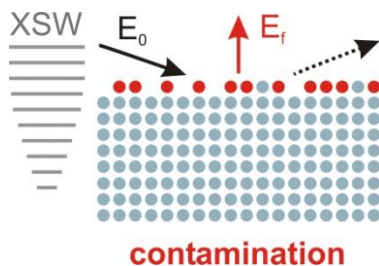
$$\frac{m_i}{F_I} = \frac{-1}{\mu_{tot,i}} \ln \left\{ 1 - \frac{P_i}{P_{0,Wsurf} \tau_{i,E_0} Q \frac{\Omega_{det}}{4\pi} \frac{1}{\sin \psi_{in}} \frac{1}{\mu_{tot,i}}} \right\}$$

E_0 photon energy of the incident (excitation) radiation

$P_0 = S_0 / \sigma_{diode,E_0}$ radiant power of the incident radiation

S_0 signal of the photodiode measuring the incident radiation

σ_{diode,E_0} spectral responsivity of the photodiode



Reference-free quantitation in SR-TXRF analysis

mass deposition m_i / F_I of the element i with unit area F_I

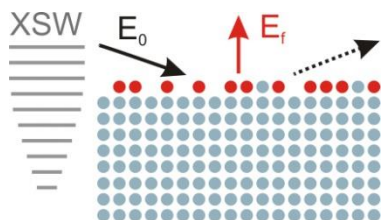
$$\frac{m_i}{F_I} = \frac{-1}{\mu_{tot,i}} \ln \left\{ 1 - \frac{P_i}{P_{0,Wsurf} \tau_{i,E_0} Q \frac{\Omega_{det}}{4\pi} \frac{1}{\sin \psi_{in}} \frac{1}{\mu_{tot,i}}} \right\}$$

ω_{Xi} fluorescence yield of the absorption edge Xi (of the element i)

$g_{l,Xi}$ transition probability of the fluorescence line l belonging to Xi

j_{Xi} jump ratio at the absorption edge Xi

$$Q = \omega_{Xi} g_{l,Xi} (j_{Xi} - 1) / j_{Xi}$$



contamination

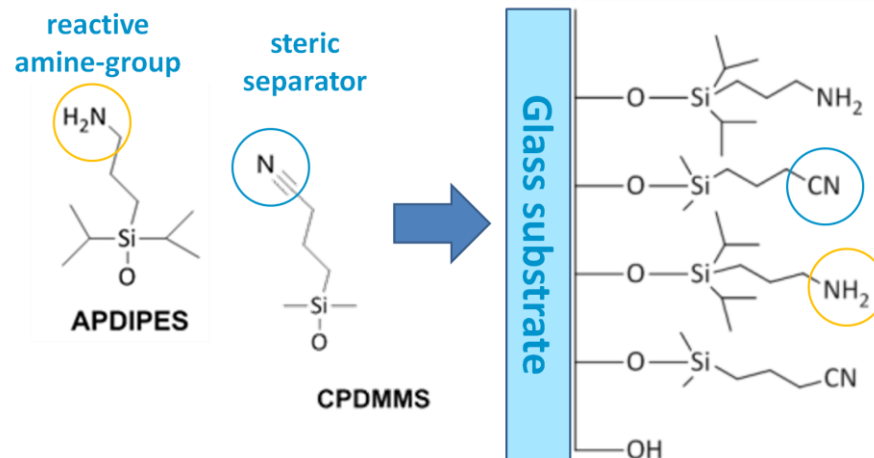
Analysis of contamination on novel materials
(Ge, SOI, InGaAs, ...) or of nanolayered
systems (buried interfaces – photovoltaics)

→ calculation of the x-ray standing wave field

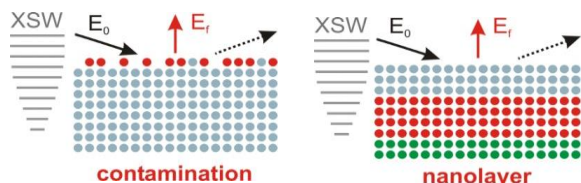
Traceable quantification of functionalized surfaces by means of reference-free TXRF analysis

- Organo-silanes for surface functionalization : aminated monolayers with a controlled density of functional and reactive groups
- determination of molecular surface density by means of reference-free TXRF analysis
- traceable quantification based on usage of specific elements as markers (here: nitrogen)
- validation of other methods, e.g. XPS

Organo-silanes for surface functionalization:

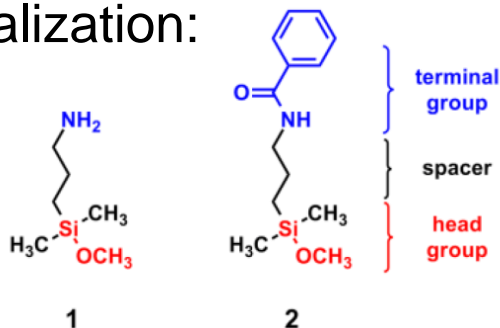


| Samples | Silane density molecules/nm ² |
|----------------------|--|
| 100 % APDIPES | 2.3 |
| 1:1 CPDMMS / APDIPES | 2.4 |
| 100 % CPDMMS | 2.1 |
| pure glass | - |



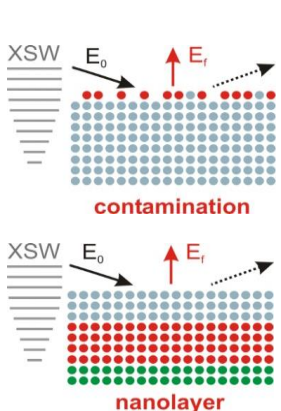
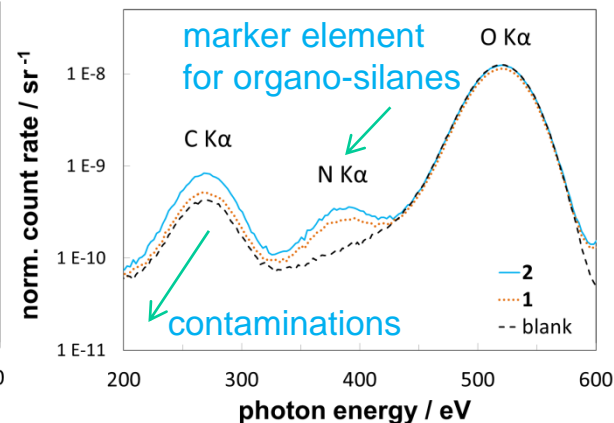
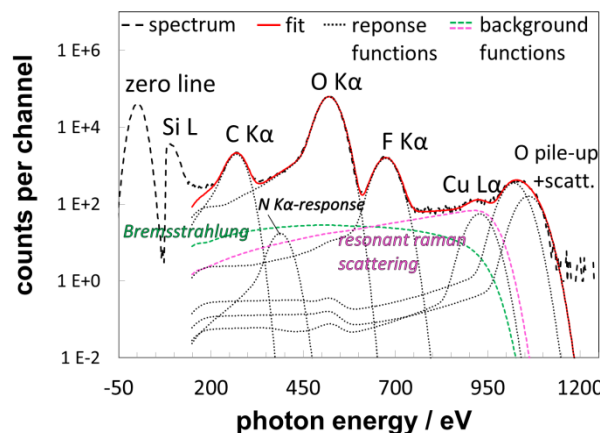
Traceable quantification of functionalized surfaces by means of reference-free TXRF analysis

- Single organo-silanes for surface functionalization:



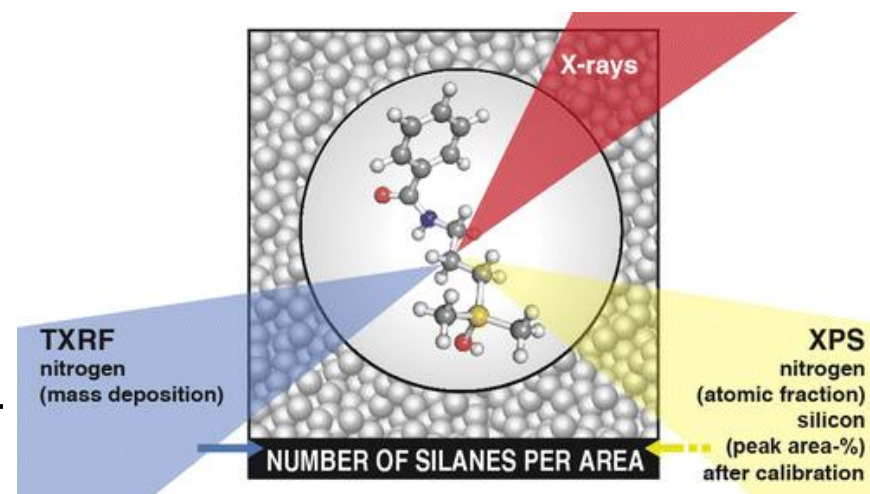
- molecular surface density as revealed by reference-free TXRF
- traceable quantification based on specific elements as **marker** (nitrogen)

Spectral deconvolution:



| layer | TXRF | | |
|-------|---------------------------------|--|--------------------------------|
| | nitrogen [$\frac{ng}{cm}$] | silane areic density [$\frac{molecules}{nm^2}$] | thickness ¹ [nm] |
| 1 | 5.9±1.8 | 2.5±0.8 | 0.6±0.2 |
| 2 | 8.9±2.7 | 3.8±1.1 | 1.4±0.5 |

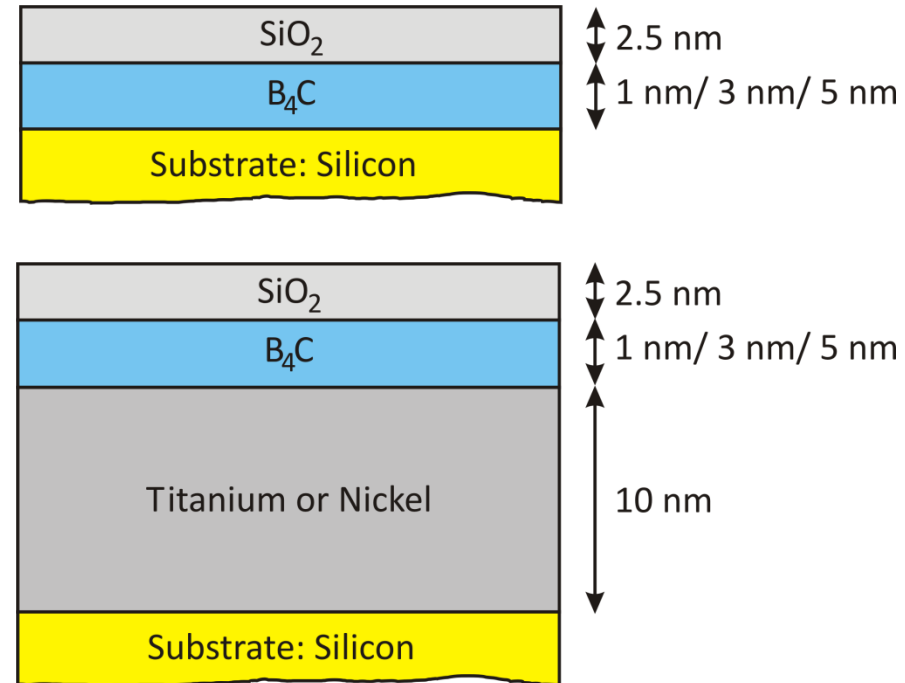
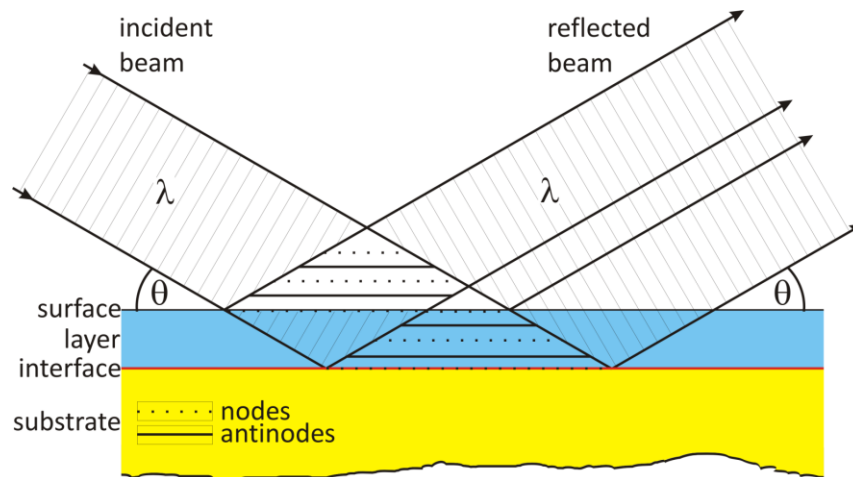
C. Streeck, A. Nutsch



Anal. Chem. 87, 10117 (2015)

Reference-free XRF and grazing-incidence XRF of buried nanolayers - layer composition and thickness

X-ray standing wave field (XSW)

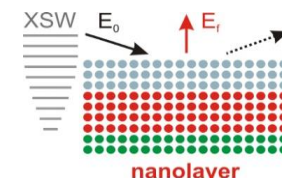


design of samples: total-reflection of the incident beam at silicon or at the metal

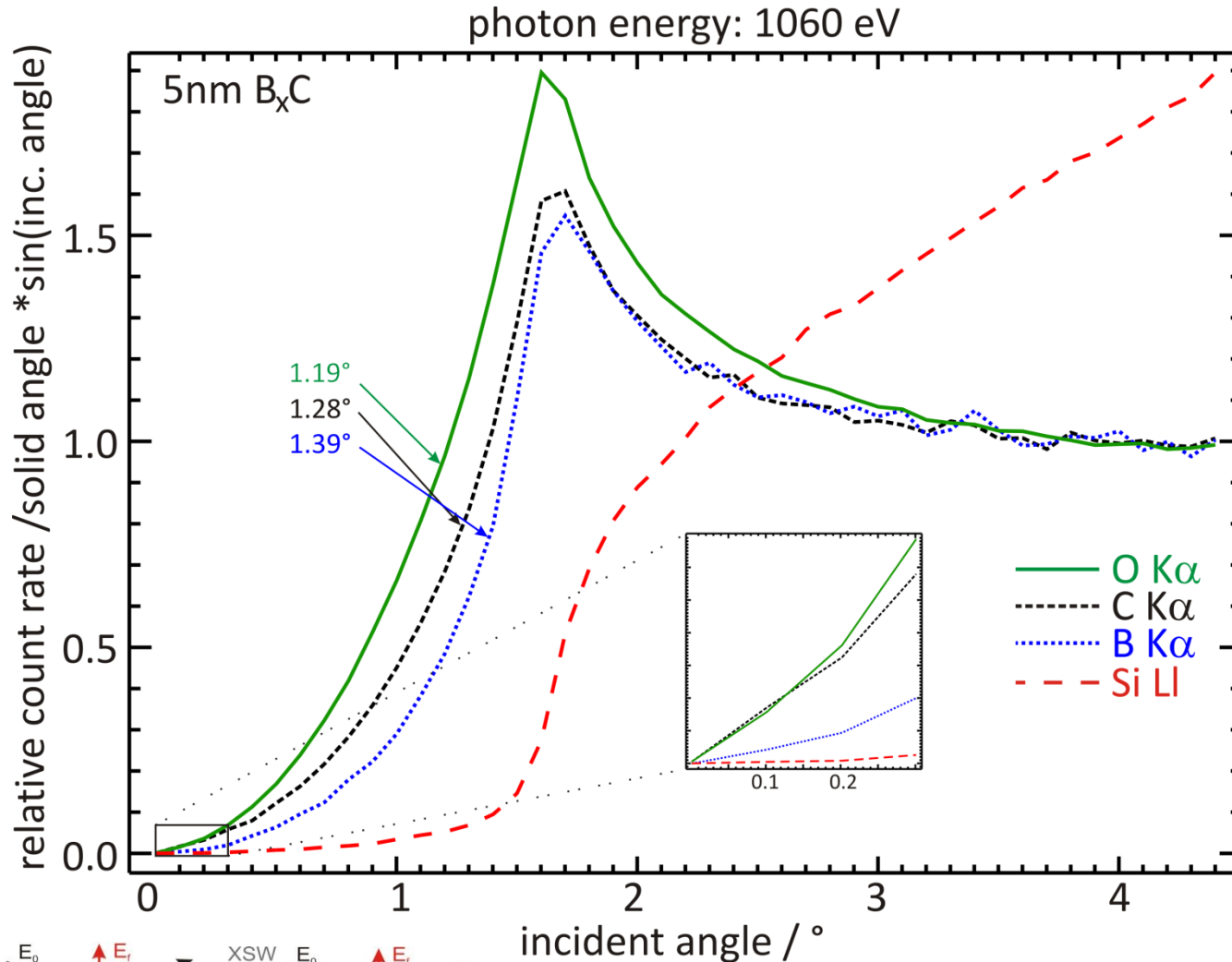
→ occurrence of the XSW in boron carbide layer

objective: determination of the boron carbide layer composition and thickness

→ comparison of XRF and GIXRF quantification



Reference-free XRF and grazing-incidence XRF of buried nanolayers - layer composition and thickness



depth-dependent modification of the excitation radiation due to XSW



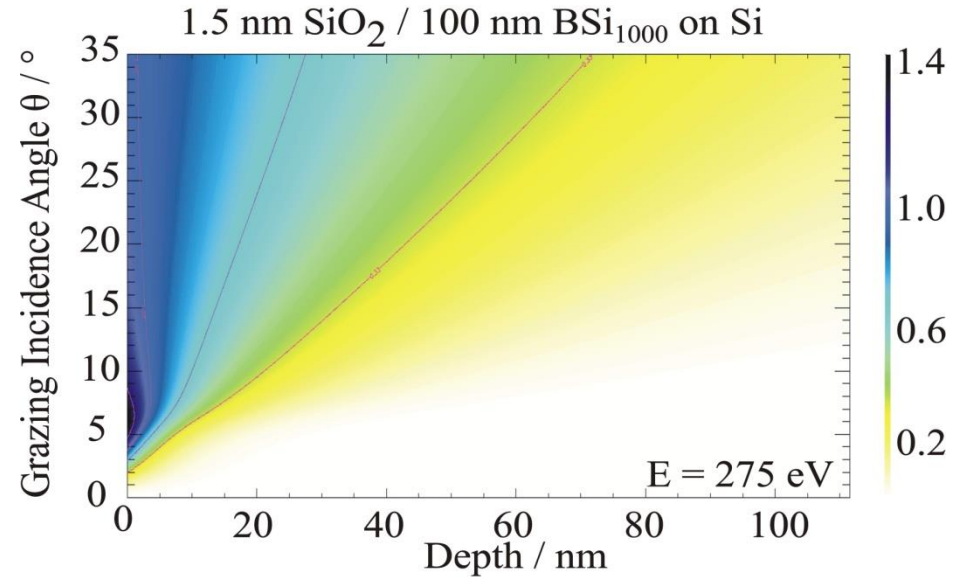
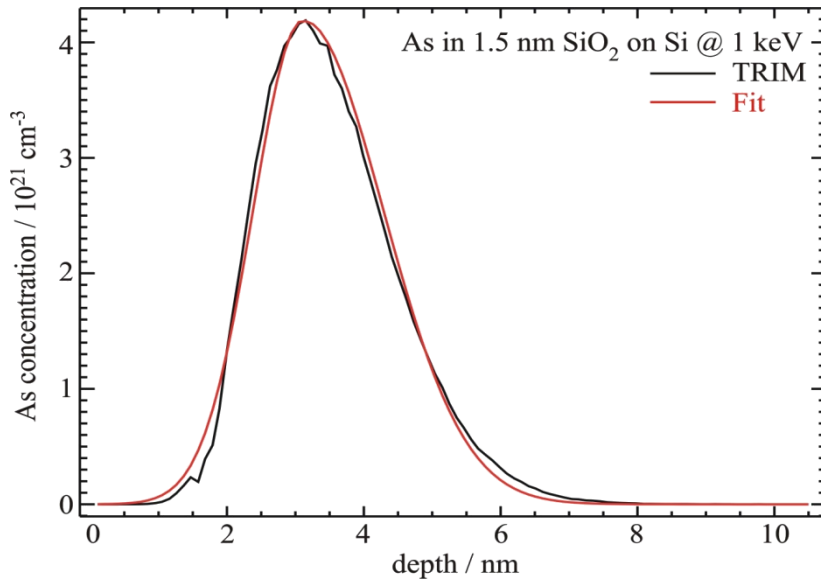
reveal information about the sequence of the layers

1. oxygen
2. carbon
3. boron
4. silicon (substrate)

carbon contamination at surface recorded



GIXRF analysis of B and As implantation profiles

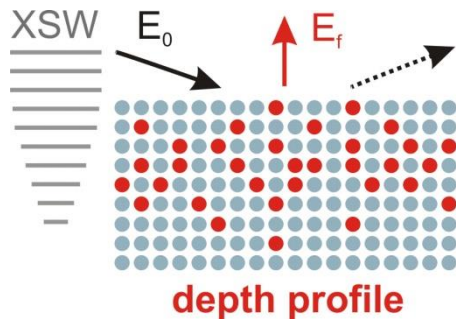


fundamental and instrumental parameters

depth distribution of the implant

X-ray Standing Wave field distribution

absorption term



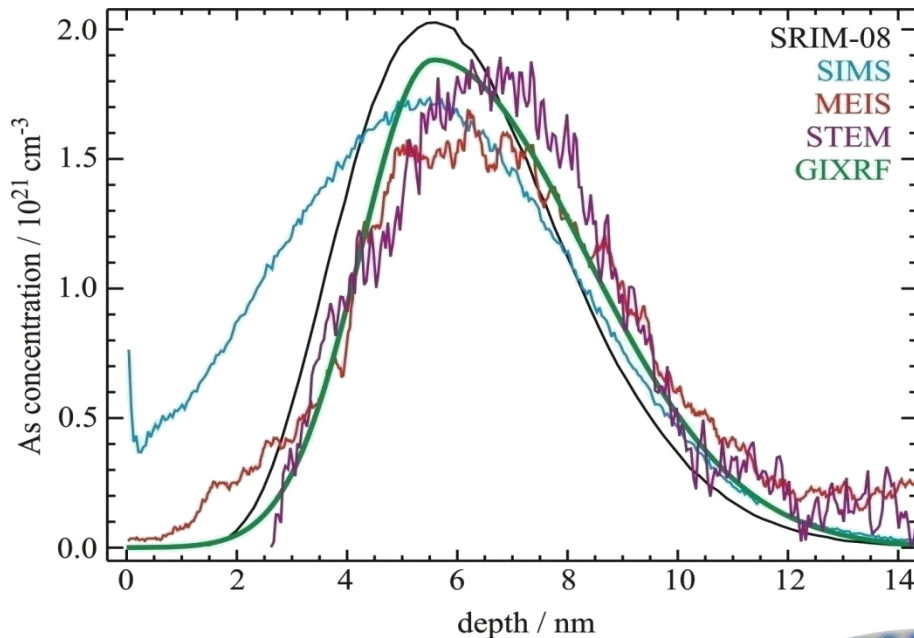
$$F_{Imp}(\theta) = G \int_0^{t_{max}} P_{Imp}(t) \cdot I_{XSW}(t, \theta, E_0) \cdot \left(e^{-\frac{t \rho \mu_{tot}(t)}{\sin \theta_{det}}} \right) dt$$

P. Hönicke

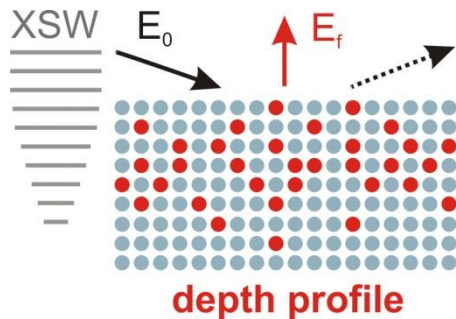
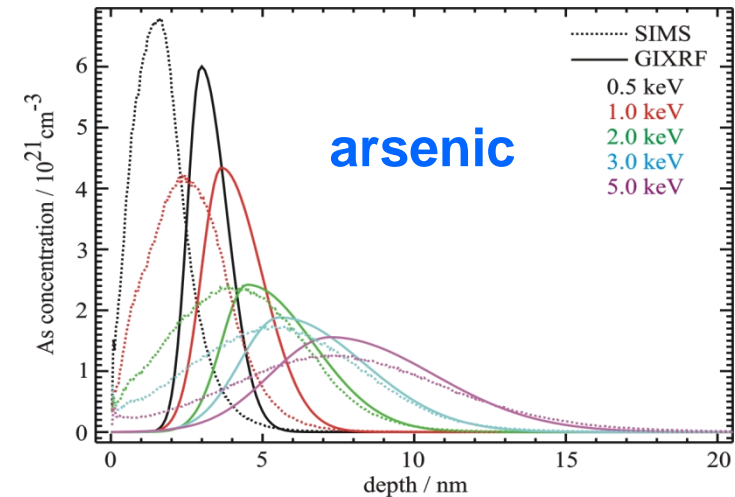
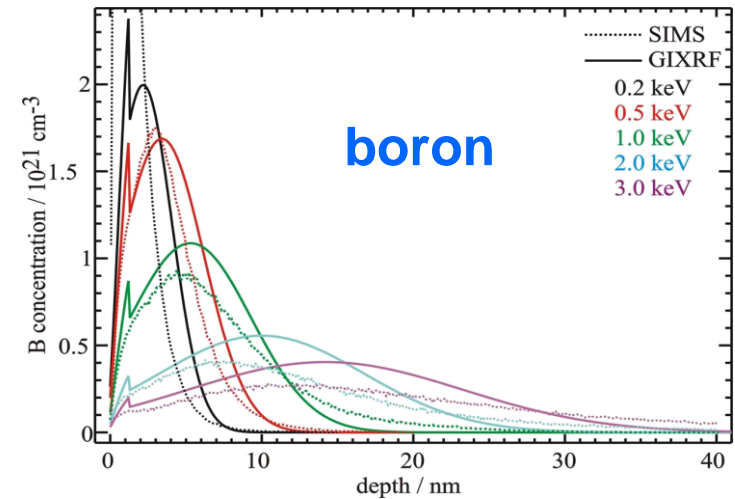
Anal. Bioanal. Chem. **396**, 2825 (2010)

GIXRF analysis of B and As implantation profiles

Comparison of GIXRF results on arsenic samples to SIMS, MEIS and STEM



Comparison of GIXRF results to SIMS



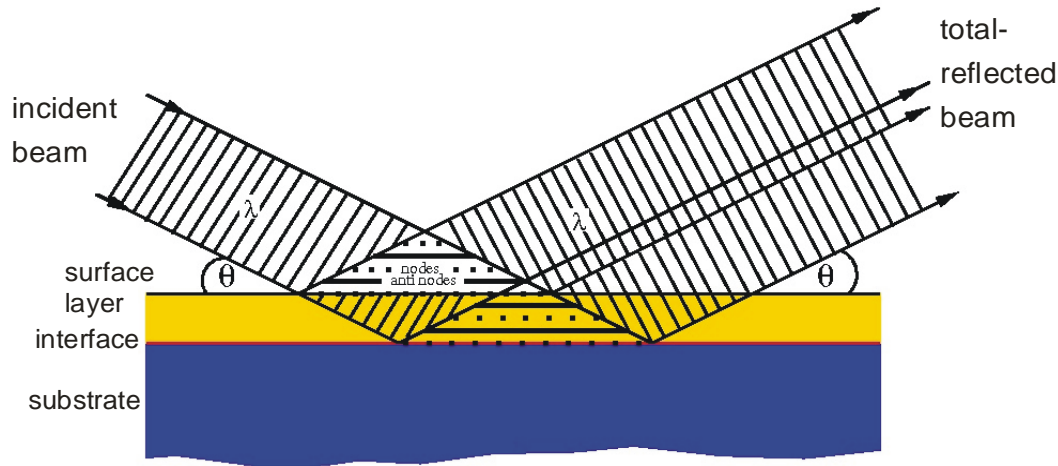
D. Giubertoni (FBK)

J. van den Berg (Univ. Salford)

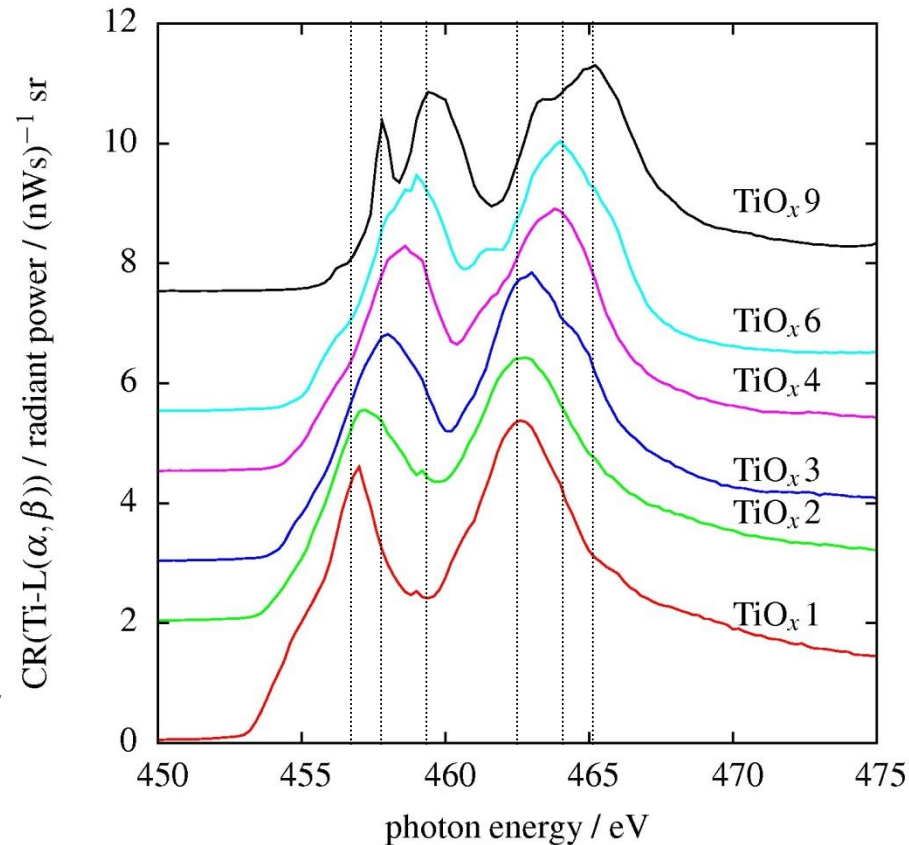
P. Hönicke

Anal. Bioanal. Chem. **396**, 2825 (2010)

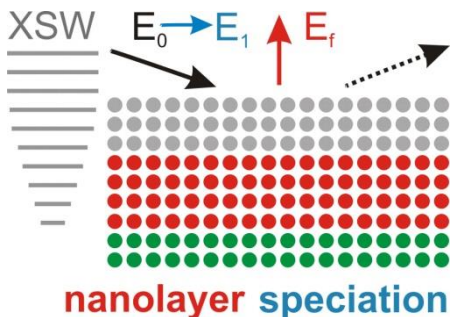
Speciation of buried nanolayers by GIXRF-NEXAFS



GIXRF-NEXAFS at the Ti-L_{iii,ii} edges



- composition and speciation of buried nanolayers
- higher information depth (>> 5nm) than XPS
- parallel variation of incident angle and photon energy



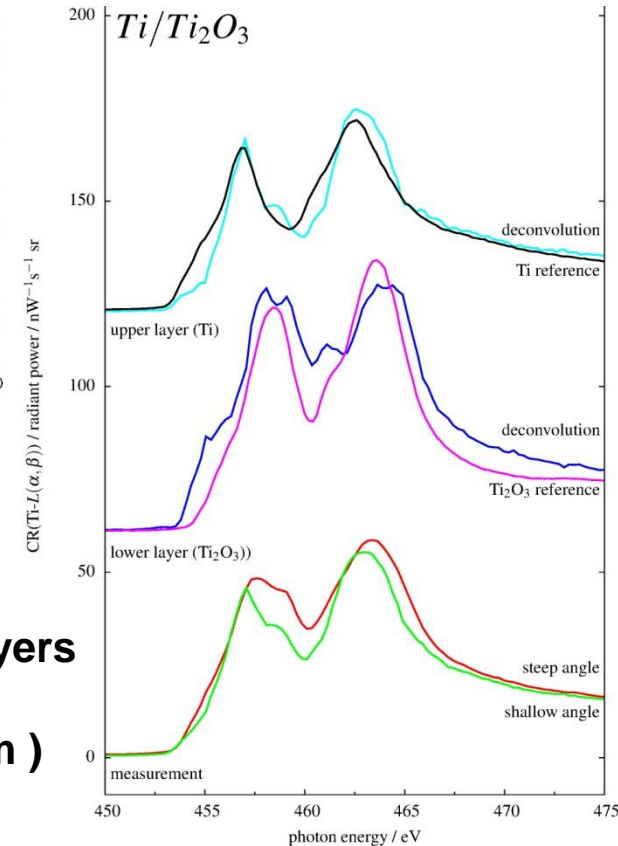
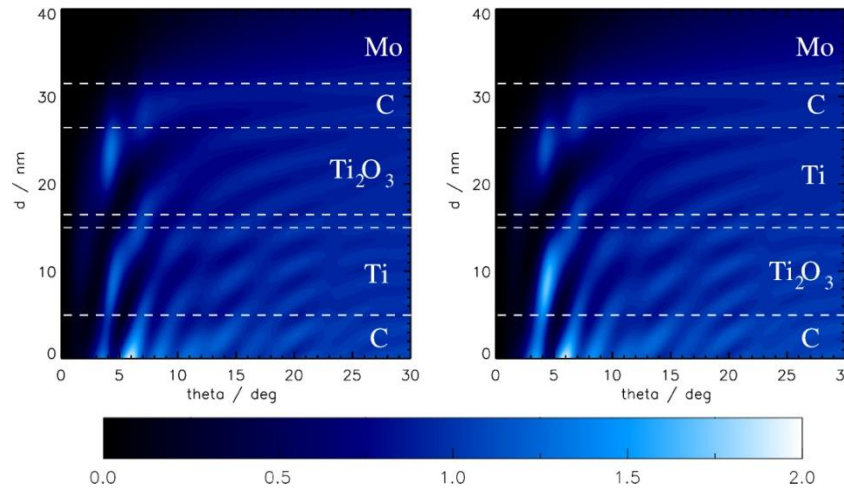
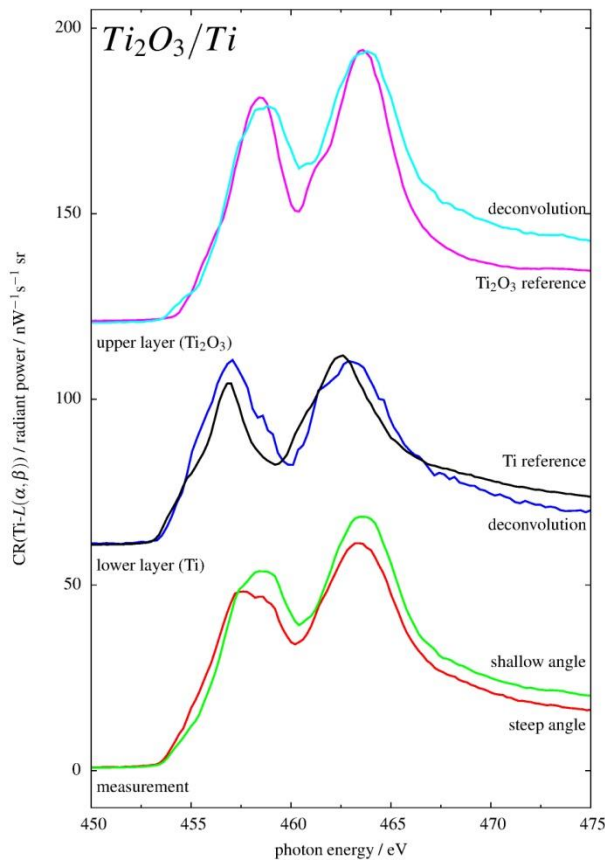
B. Pollakowski

Phys. Rev. B **77**, 235408 (2008)

Anal. Chem. **85**, 193 (2013)

speciation of buried Ti oxide nanolayers
(the degree of oxidation scales with indices)

Speciation depth profiling by GIXRF-NEXAFS

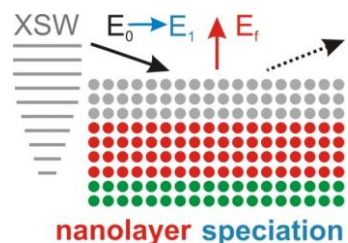


→ speciation of $Ti_{x_1}O_{y_1} / Ti_{x_2}O_{y_2}$ nanolayers

→ high information depth (up to 500 nm)

→ simultaneous variation of angle of

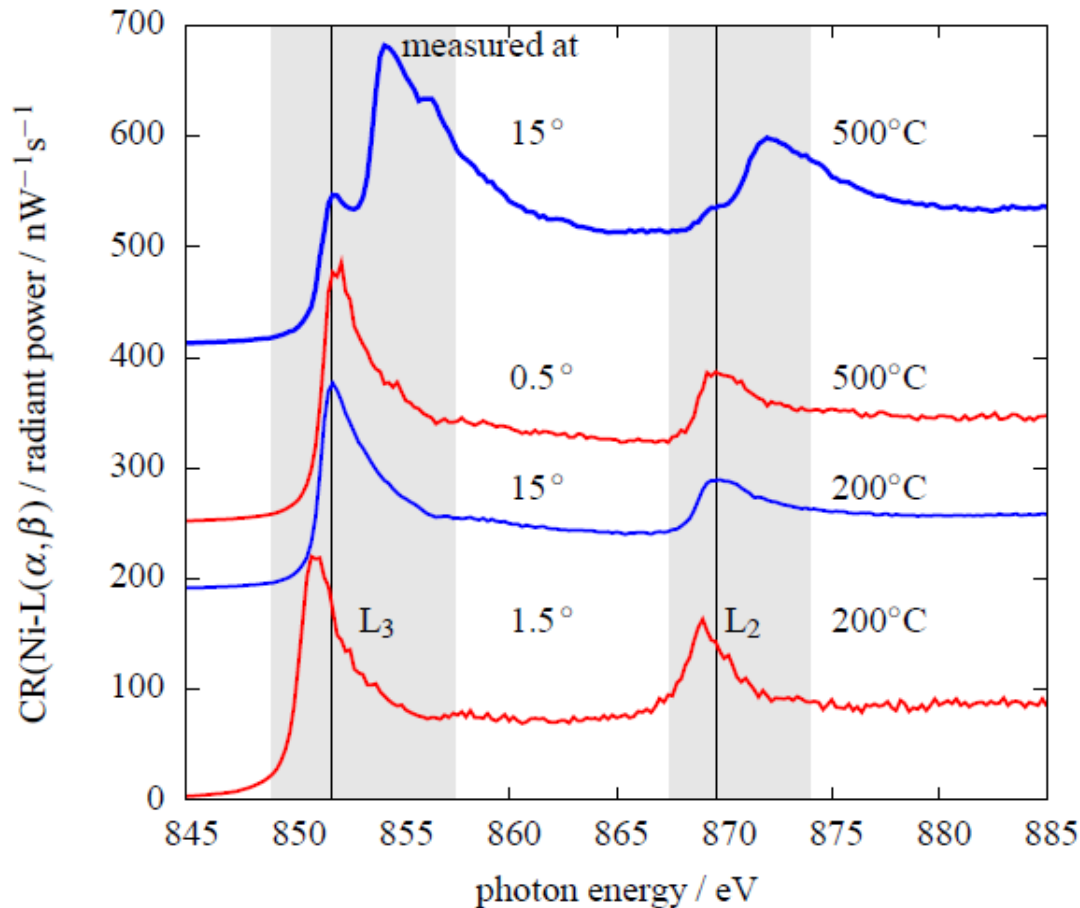
incidence and of the photon energy



B. Pollakowski

Anal. Chem. **87**, 7705 (2015)

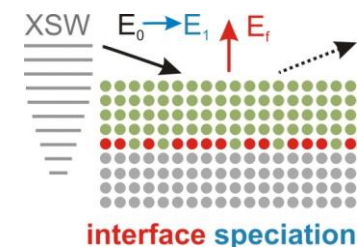
Speciation of buried interfaces by GIXRF-NEXAFS



- **Comparison** between a **shallow** and a **steep** angle
- Interface observable: Ni-C, Ni-N or Ni-Si bonds possible

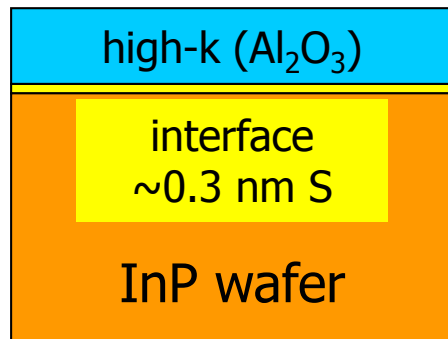
B. Pollakowski

Anal. Chem. **85**, 193 (2013)

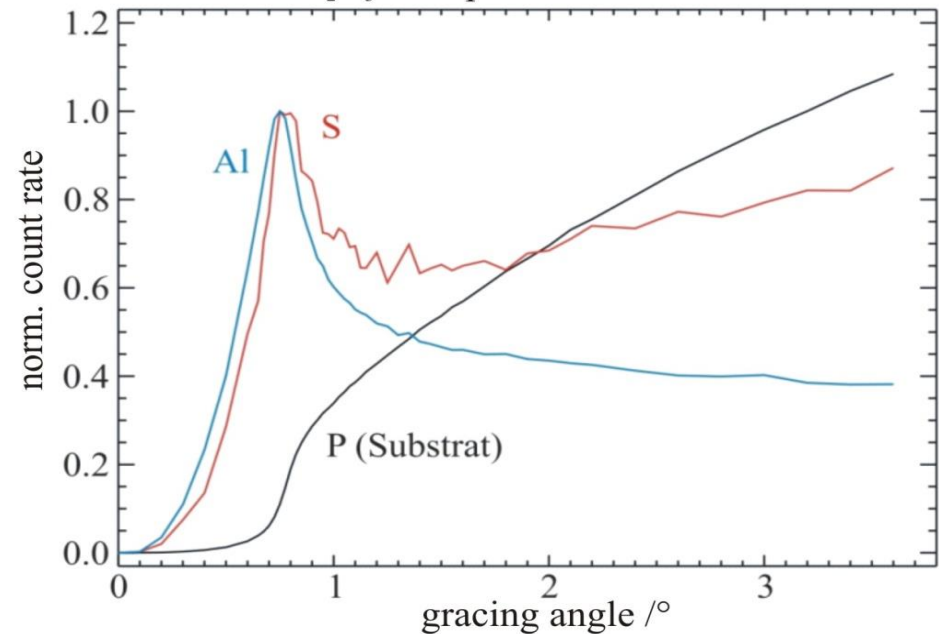


Quantitative characterization of nanoelectronics

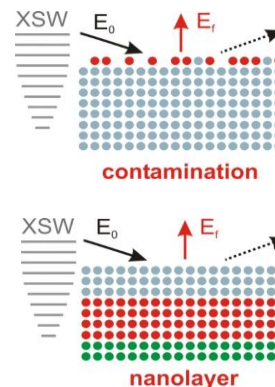
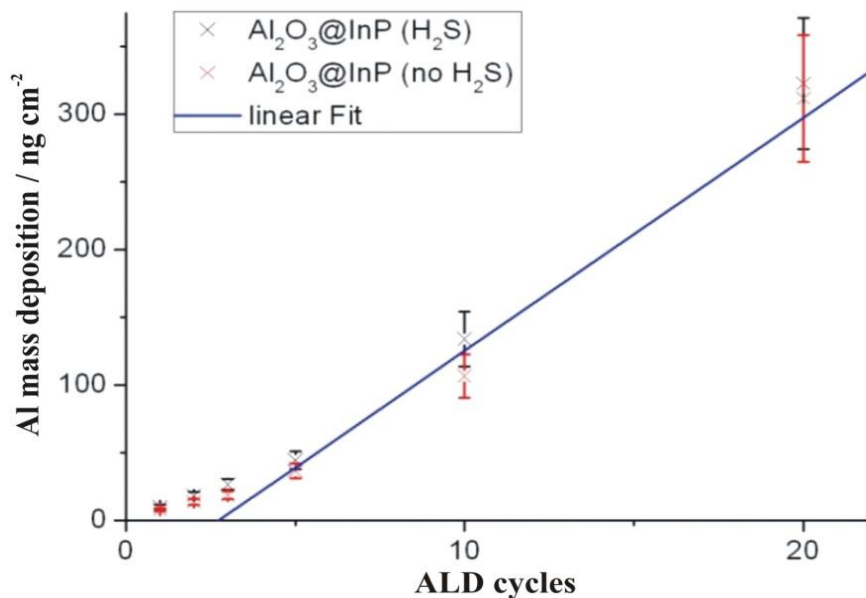
Optimization of high-k nanolayer fabrication



3 nm Al₂O₃ on S passivated INP substrate



Quantification of the ALD growth rate

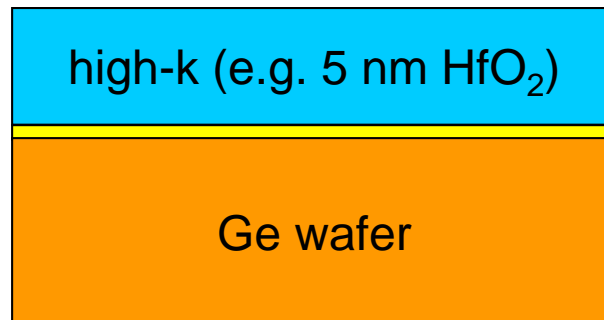
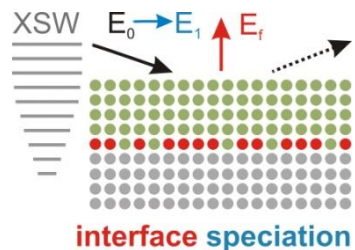
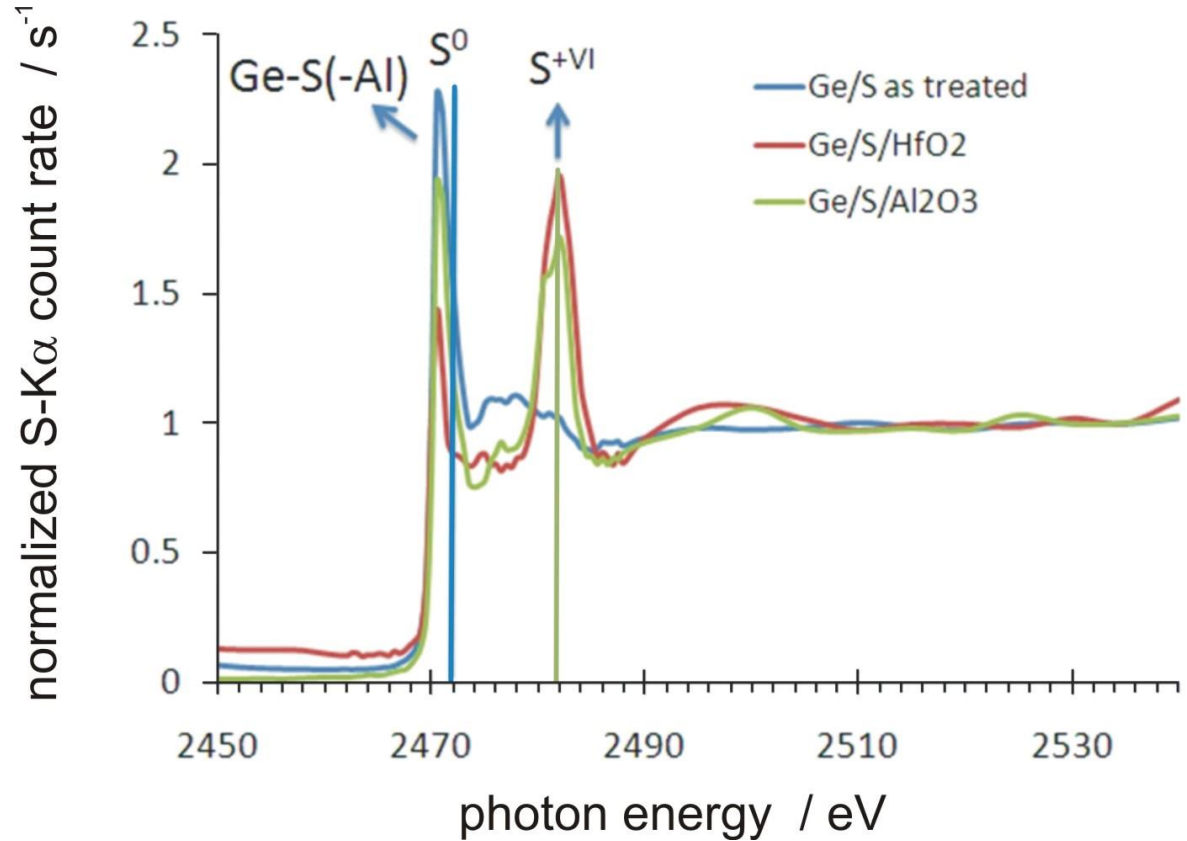


linear growth on S passivated InP substrate after the 3rd ALD cycle

J. Vac. Sci. Technol. A **30**, 01A127 (2012)

Quantitative interface characterization and speciation

XAFS speciation of the S passivated interface as treated and for two high k cap layer



passivated interface
(S monolayer ~0.3 nm)

M.Müller

J. Electrochem. Soc. **158**, H1090 (2011)



GIXRF-NEXAFS at thin-film Si photovoltaics: probing the chemical state of buried interfaces

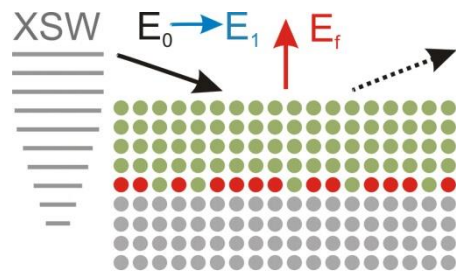
GIXRF-NEXAFS requirements:

- transmission through a-Si layer
- total reflection at interface

Si:P - Si doped with 0,2 at% P

ZnO:Al - ca. 2 at.% Al

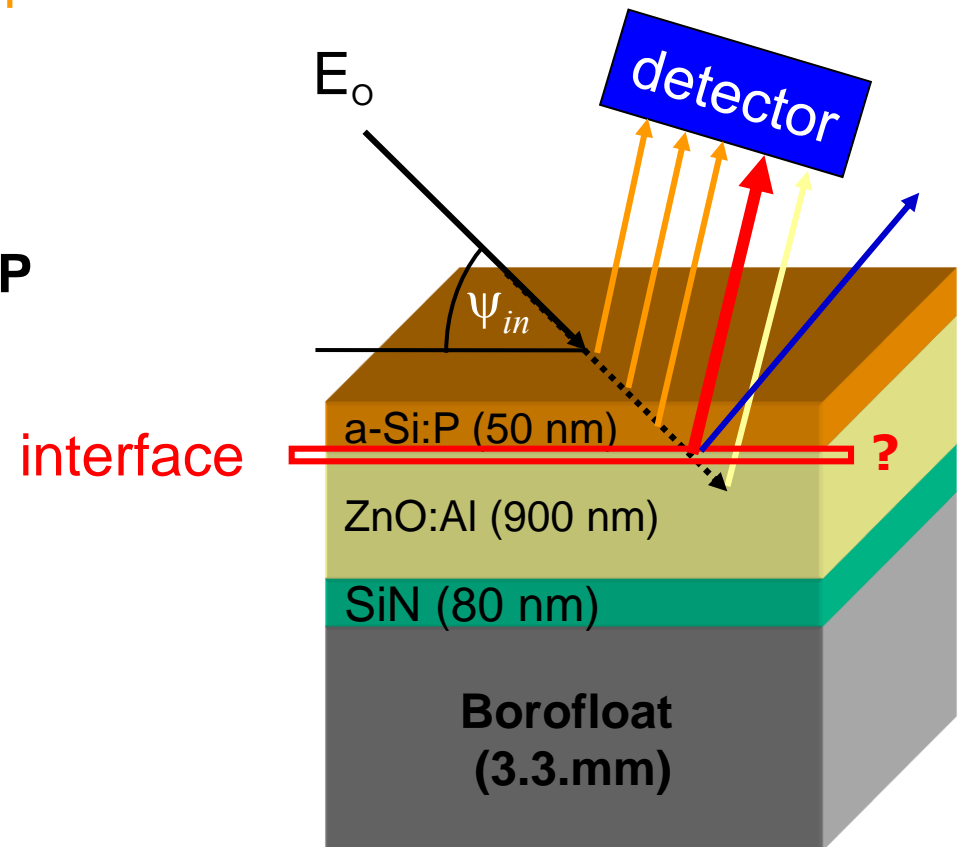
SiN - Si:N = 3:4



interface speciation

M. Pagels,
TUB / HZB

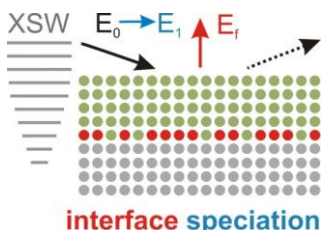
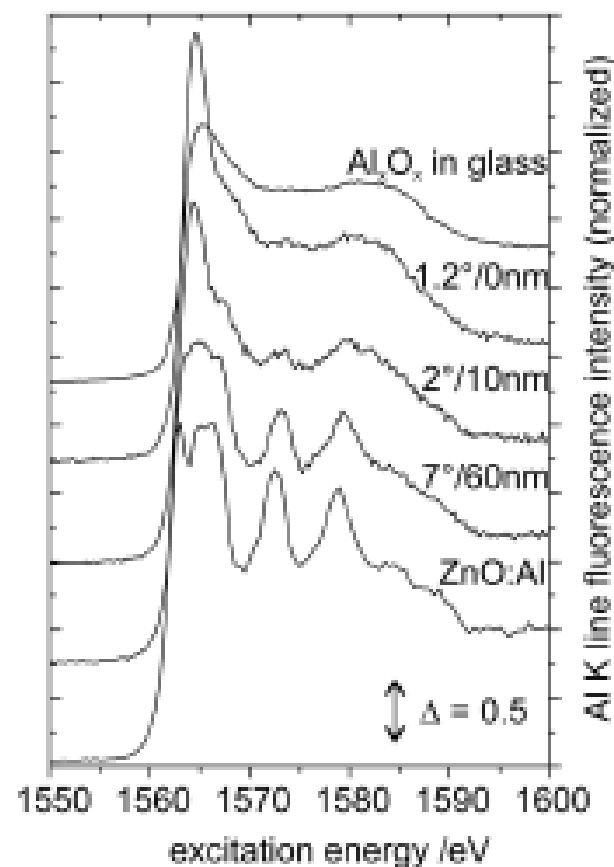
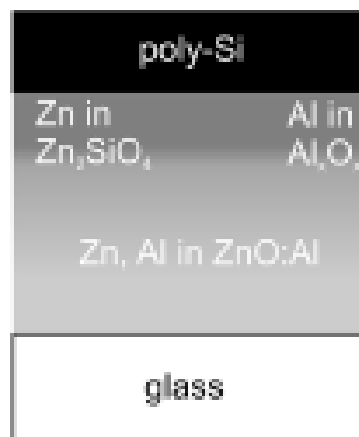
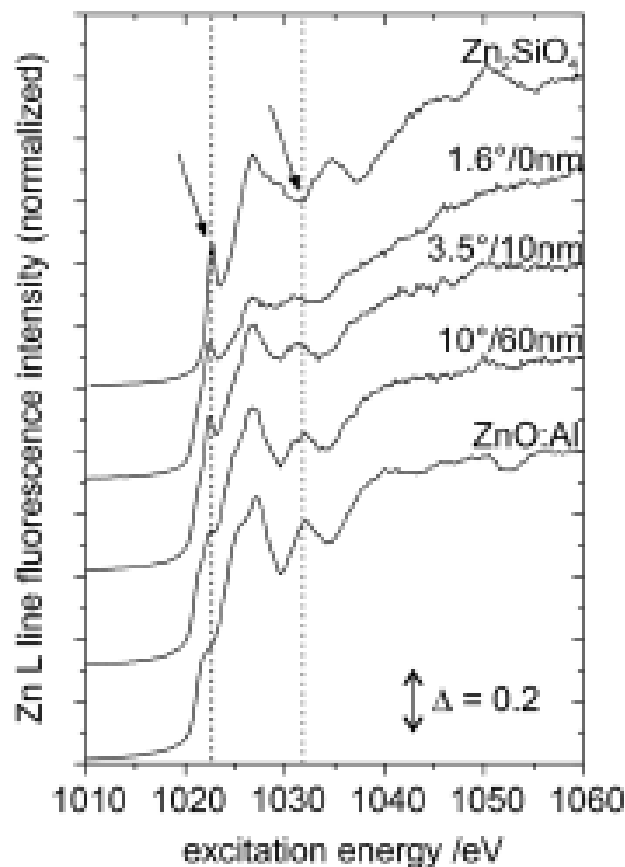
B. Pollakowski



NIMB 268, 370 (2010)

GIXRF-NEXAFS at thin-film Si photovoltaics: probing the chemical state of buried interfaces

NEXAFS investigations at the Zn-L_{iii,ii} and Al-K edges



M. Pagels, TUB / HZB

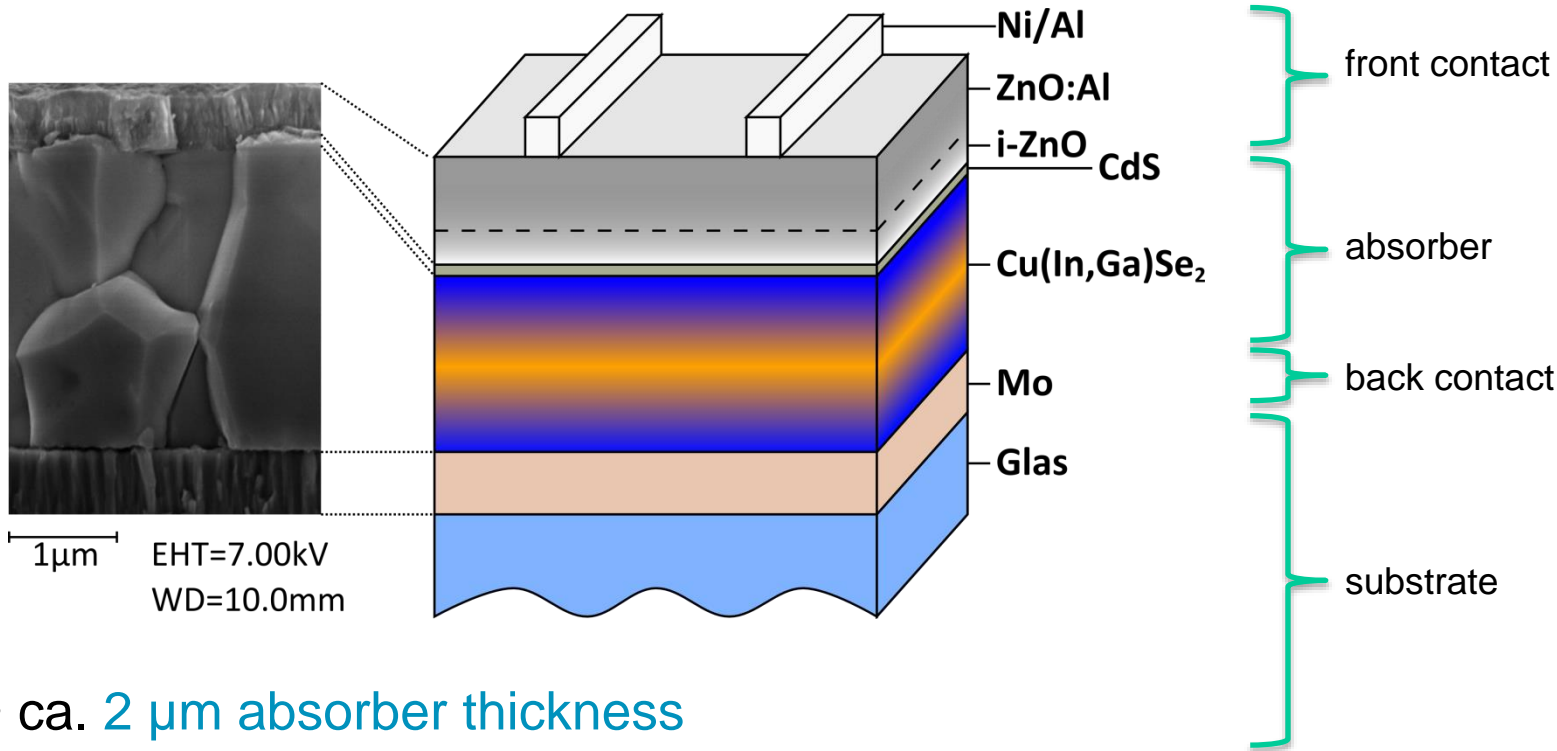
C. Becker, HZB

B. Pollakowski

J. Appl. Phys. **113**, 044519 (2013)

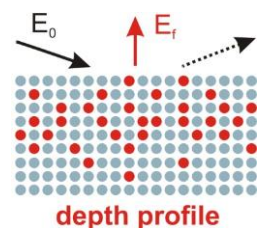
Elemental depth profiling of CIGS photovoltaics by GIXRF using calibrated instrumentation

Cu(In,Ga)Se₂ absorber for thin film solar cells



- ca. 2 μm absorber thickness

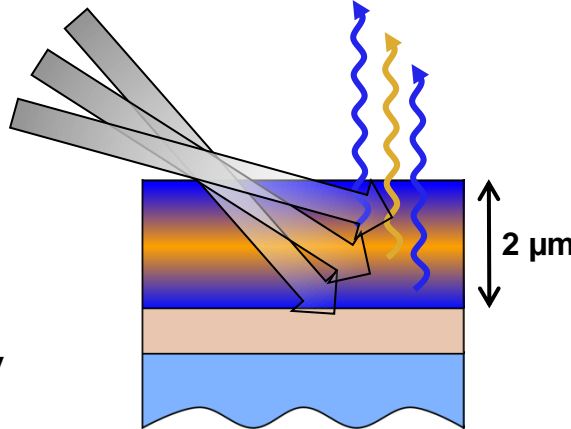
- inhomogeneous element depth distribution of In and Ga influences the efficiency



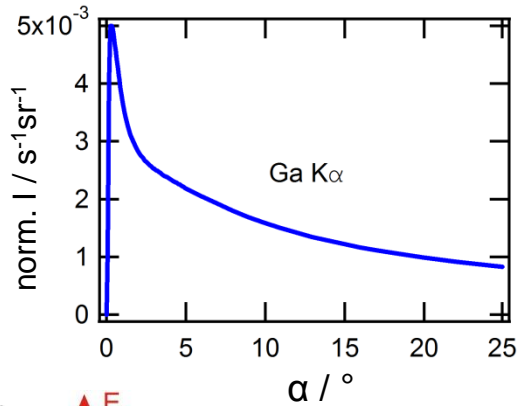
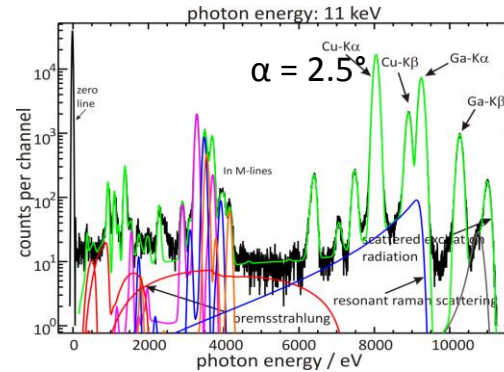
Elemental depth profiling of CIGS photovoltaics by GIXRF using calibrated instrumentation

Increasing information depth with increasing incidence angle

Fluorescence intensity in dependence of the angle of incidence



XRF-spectrum

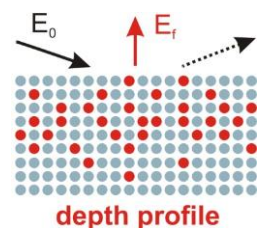
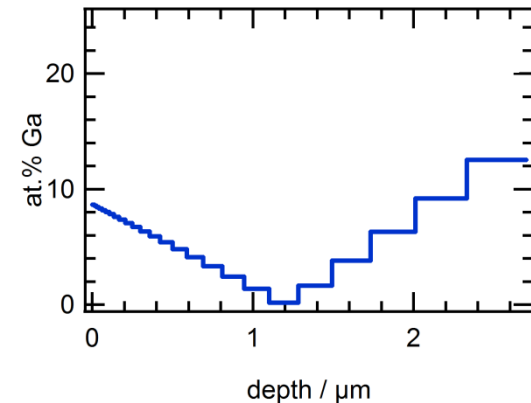


GIXRF

Non-destructive access to the elemental depth profile

Fundamental parameter-based quantification

Elemental depth profile





Elemental depth profiling of CIGS photovoltaics by GIXRF using calibrated instrumentation

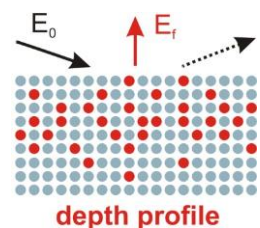
BIPM Pilot-study CCQM-P140

CCQM-P140

SURFACE ANALYSIS

Measurement of atomic fractions in Cu(In,Ga)Se₂ Films

| Composition / at. % | Certified values  Korea Research Institute of Standards and Science | Reference-free GIXRF  |
|---------------------|---|--|
| Cu | 23.8 ± 0.6 | 24.0 ± 1.3 |
| In | 19.1 ± 0.6 | 19.3 ± 1.1 |
| Ga | 6.6 ± 0.3 | 6.3 ± 0.4 |
| Se | 50.6 ± 1.5 | 50.4 ± 2.8 |
| d / μm | ca. 2 | 2.06 ± 0.09 |



Directed development of new energy storage materials: towards in-operando XAFS speciation of cathode films

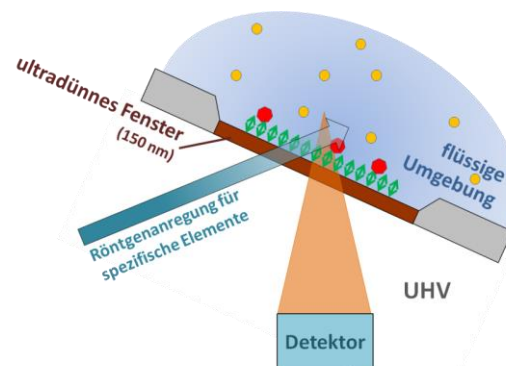
First step: No ambient air exposure

Employing a thin window argon cell for x-ray spectrometric measurements.

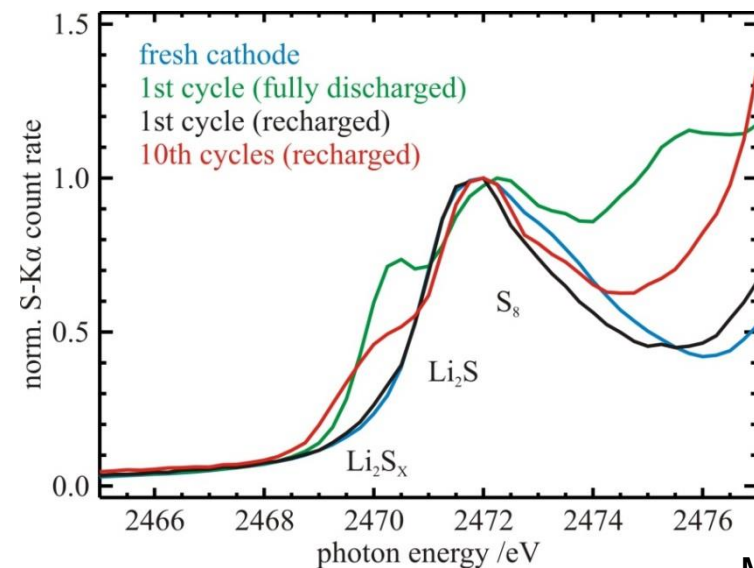
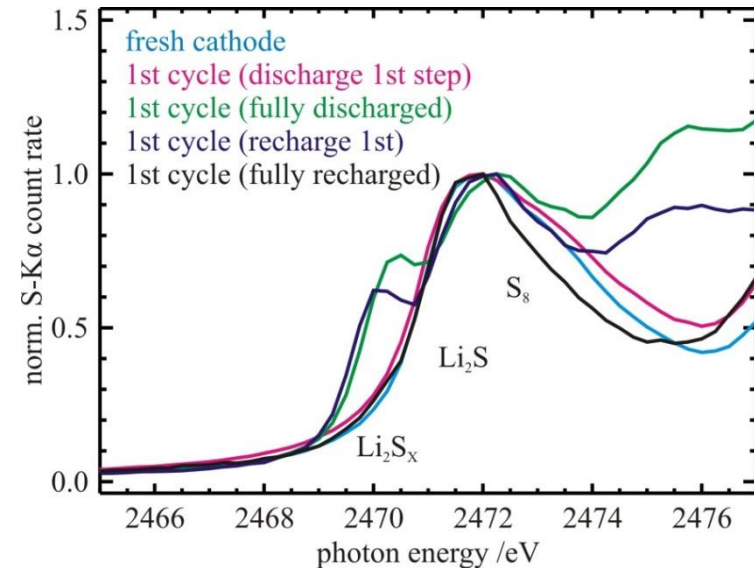
- NEXAFS measurements at different states of charge (not in-situ or operando so far)
- Formation of lithium polysulfides during discharge observed
- Polysulfides disappear during recharging
- After several recharge cycles some of the polysulfides remain

[Spectrochim. Acta B 94–95, 22 \(2014\)](#)

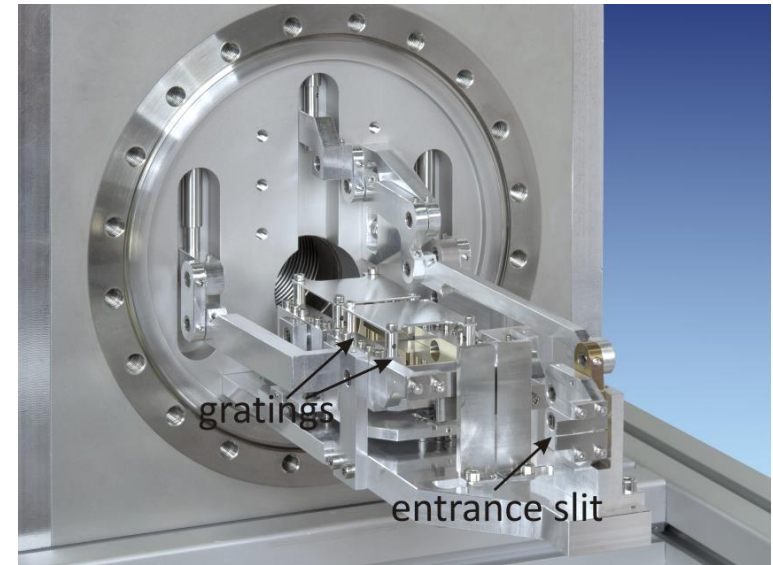
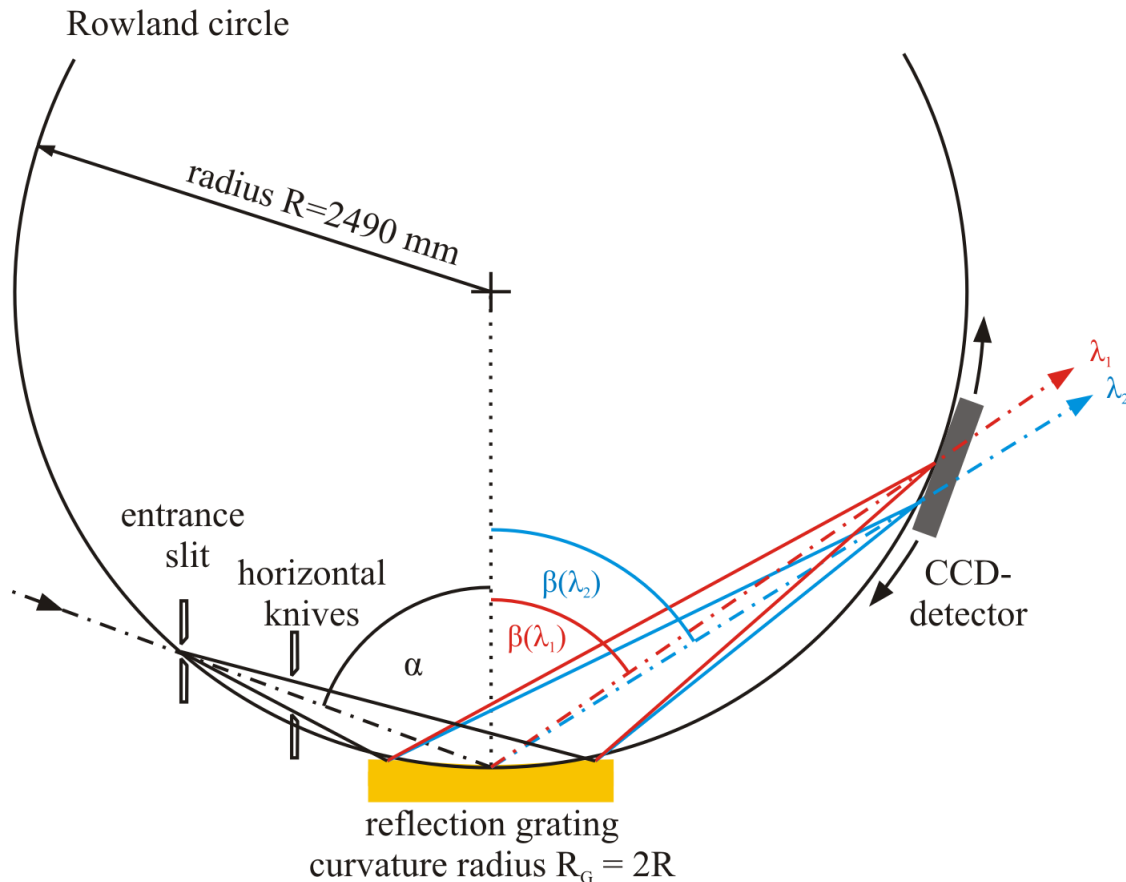
- **Patent application of liquid cell (operando studies of batteries)**





liquid-solid interfaces



Calibrated Wavelength-Dispersive Spectrometer (WDS)

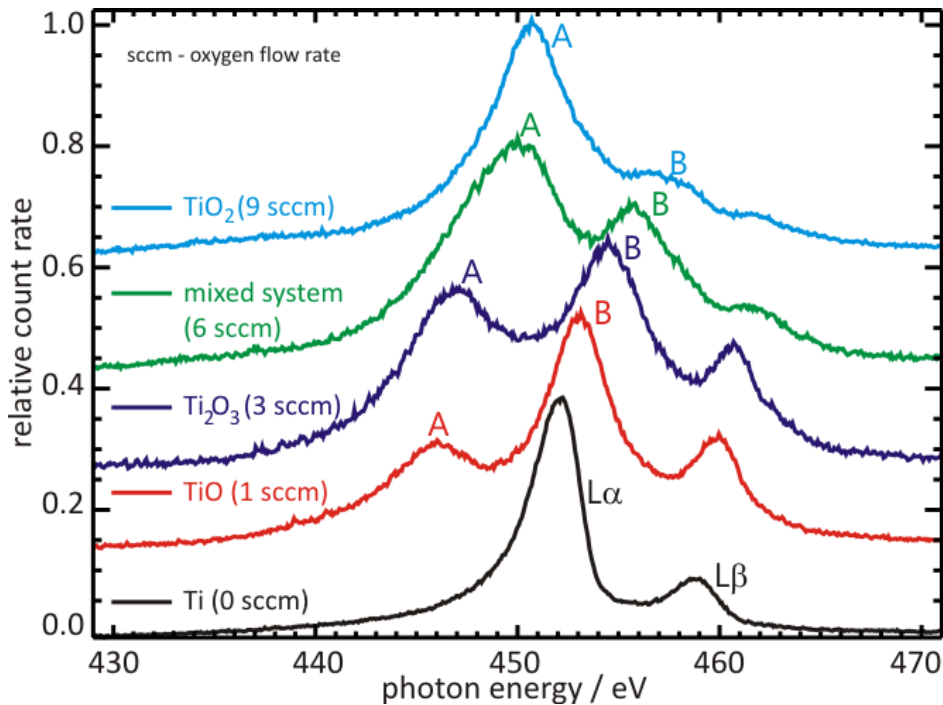


energy range:
75 eV to 1760 eV
energy resolution $E/\Delta E$:
150 to 400

- calibration  allows for the determination of fundamental parameters
- disadvantage:  low efficiency, moderate detection limit, long integration time

Chemical speciation of nanoscaled materials and

fundamental parameter determination

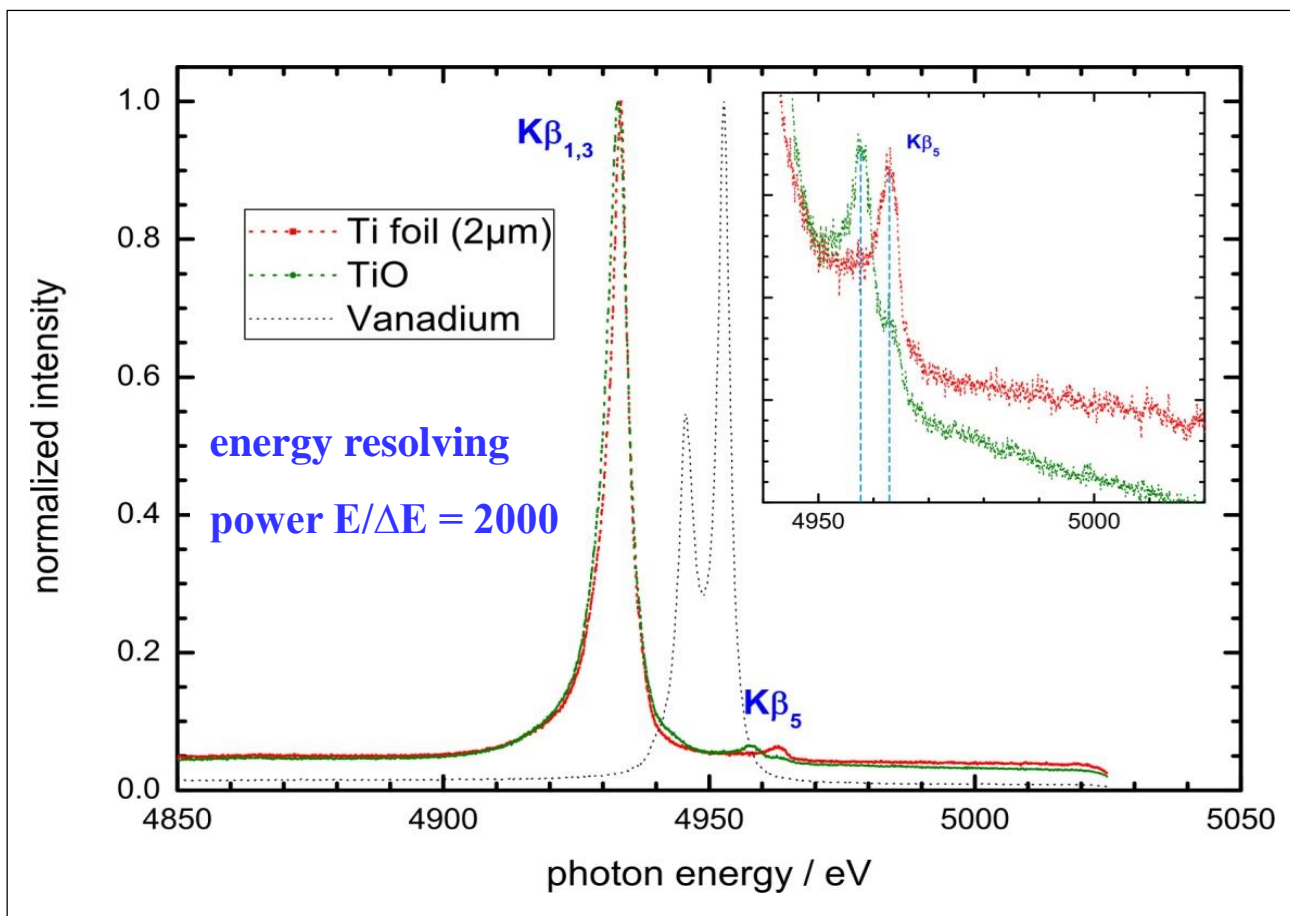


| sample | titanium L1 | uncertainties |
|--|-------------|---------------|
| metallic Ti | 0.59 | 0.06 |
| 0 sccm (Ti) | 0.59 | 0.06 |
| 1 sccm (TiO) | 0.61 | 0.09 |
| 3 sccm (Ti ₂ O ₃) | 0.57 | 0.09 |
| 6 sccm (mixed system) | 0.54 | 0.08 |
| 9 sccm (TiO ₂) | 0.46 | 0.07 |

Transition probabilities as a function of the oxidation state

Chemical speciation of titanium with a von Hamos spectrometer based on HAPG crystals

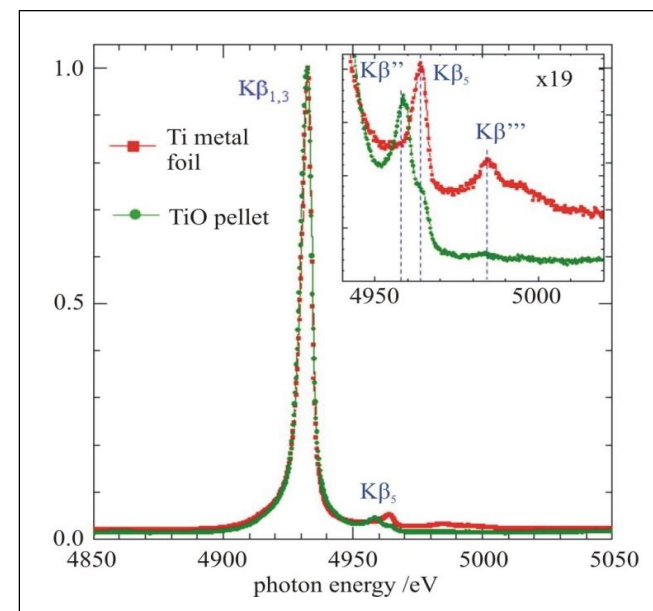
Recorded at BESSY (undispersed bending magnet radiation)



Vanadium lines used for calibration of energy scale

J. Appl. Cryst. **48**, 1381 (2015)

Measurements at SPring-8 (Japan) with a Ge crystal spectrometer with 10 keV monochromatic radiation

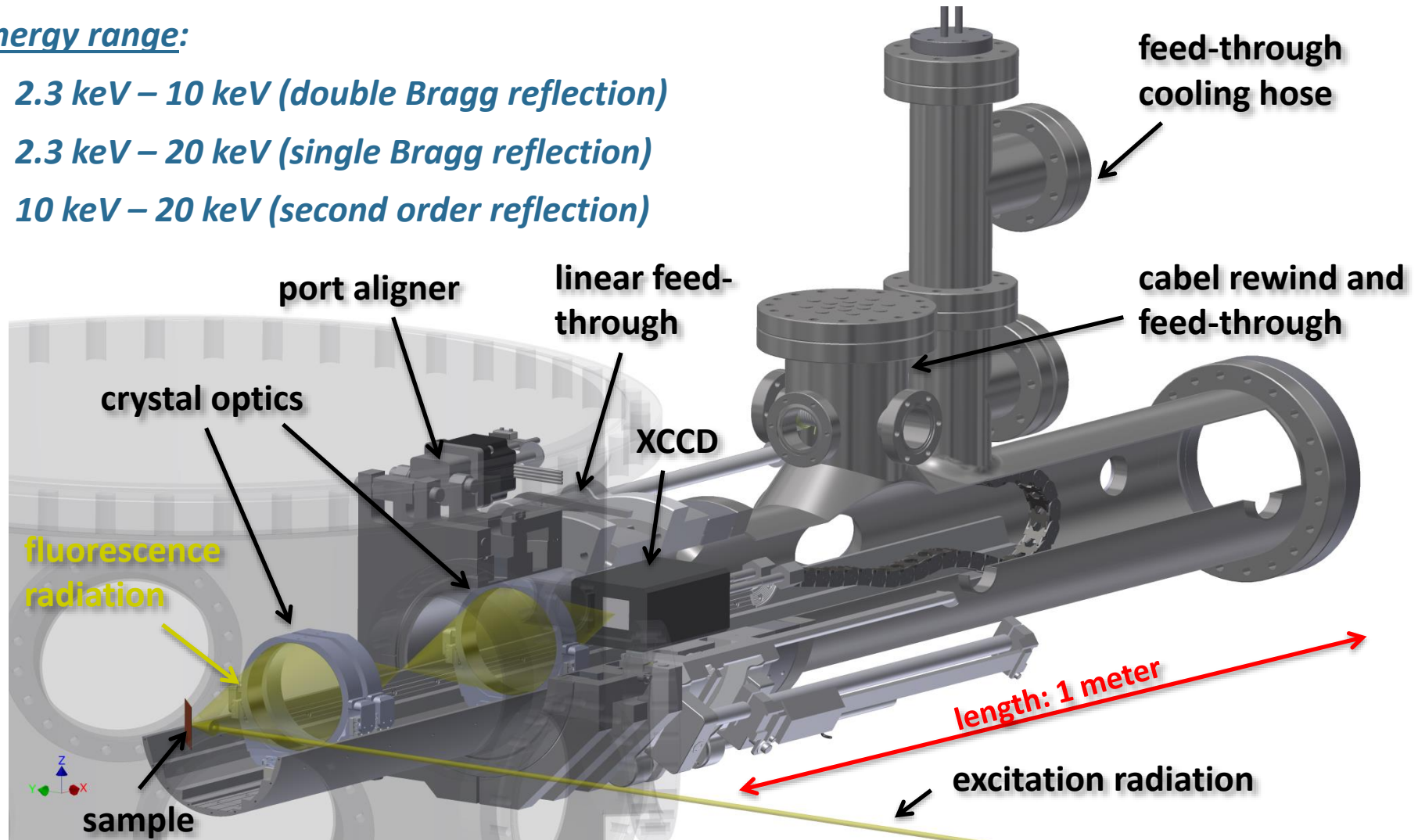


Anal. Chem. **81**, 1770 (2009)

Calibratable von Hamos spectrometer for XES

energy range:

- 2.3 keV – 10 keV (double Bragg reflection)
- 2.3 keV – 20 keV (single Bragg reflection)
- 10 keV – 20 keV (second order reflection)



Summary

- Reference-free analysis of contamination on Si and of functionalized surfaces
- Quantitative characterization of nanostructured and gradient systems ($\sim 2 \mu\text{m}$)
- Depth profiling ($\sim 500 \text{ nm}$) and interfacial speciation of nanoscaled materials
- New XRS instrumentation available at PTB, TUB, LNE-LNHB, IAEA/ELETTRA
- Calibrated high-resolution x-ray emission spectrometer and novel liquid cells

Further information on reported activities and instrumentation

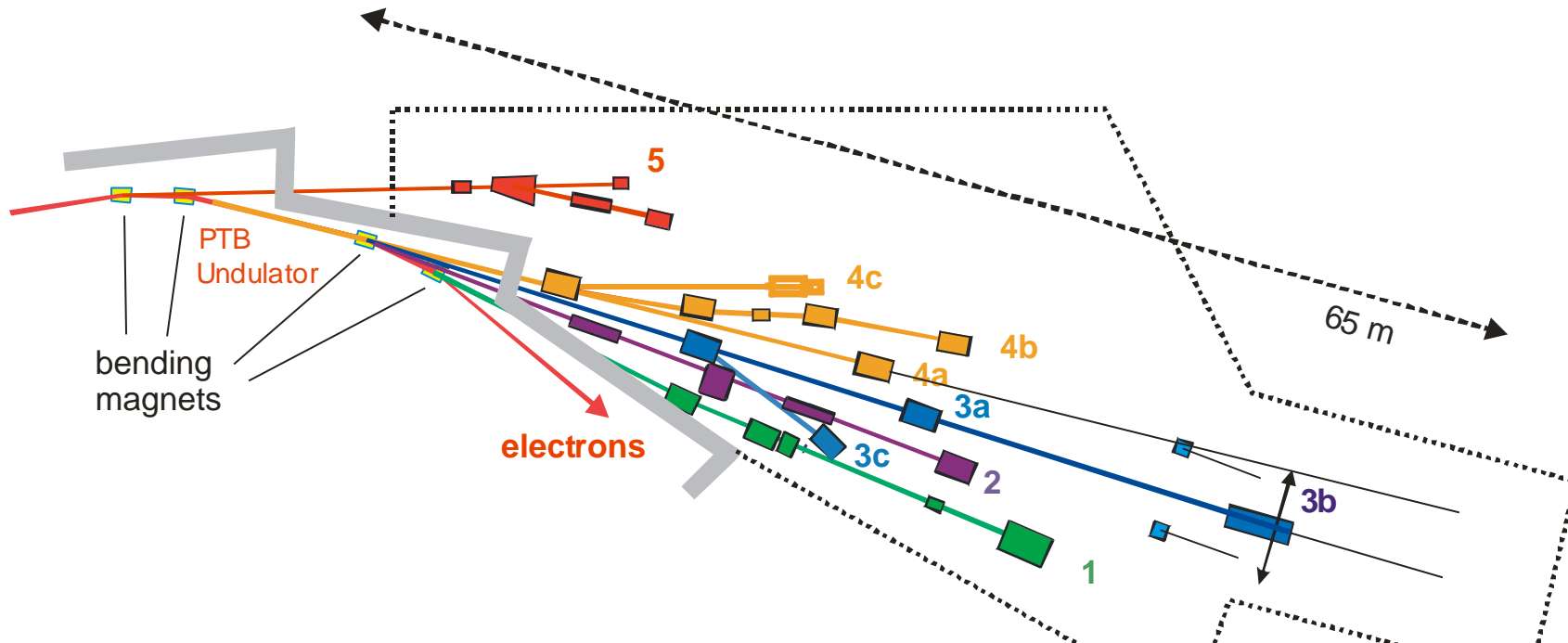
at **EMRP IND07**, **ENG53** and **NEW01** at www.EURAMET.org



Acknowledgements: IMEC, KU Leuven, IPF, LETI, LNHB, HZB, NPL, IWS, AXO, MEMC, Numonyx, Technical Universities Berlin, Darmstadt, Dresden and Ilmenau, & other industrial partners of PTB

E-MRS Symposia ,Analytical Techniques for Precise Characterization of Nanomaterials' 2014 / 2017

PTB laboratory at BESSY II: well-known synchrotron radiation for x-ray radiometry and x-ray spectrometry

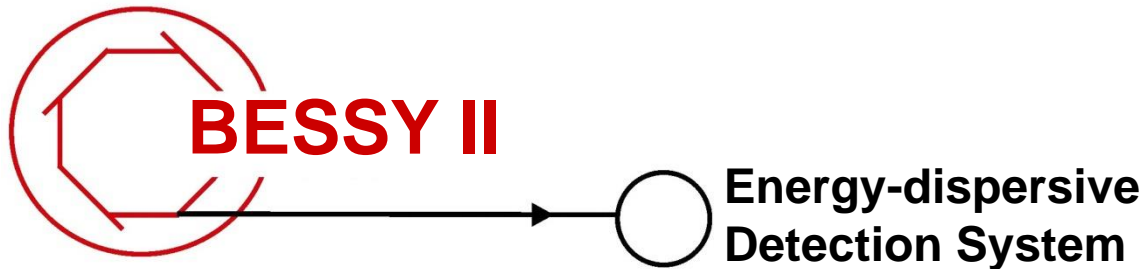


| | | | |
|-----------|--|-----------|---|
| 1 | Soft X-ray radiometry beamline 30 eV to 1900 eV (EUV XRR, detect.) | 4a | Undispersed undulator radiation |
| 2 | X-ray radiometry beamline 1.75 keV to 10 keV (XRR, XRS , XAFS) | 4b | Plane grating monochromator beamline 78 eV to 1860 eV (XRS , XAFS) |
| 3a | Undispersed bending magnet Radiation (detectors) | 4c | System metrology beamline |
| 3b | UV-VUV source characterization 3 eV to 35 eV (to be transfered to MLS) | 5 | UV-VUV radiometry beamline 3 eV to 35 eV (transfered to MLS in 2009) |
| 3c | Irradiation testing beamline | | |

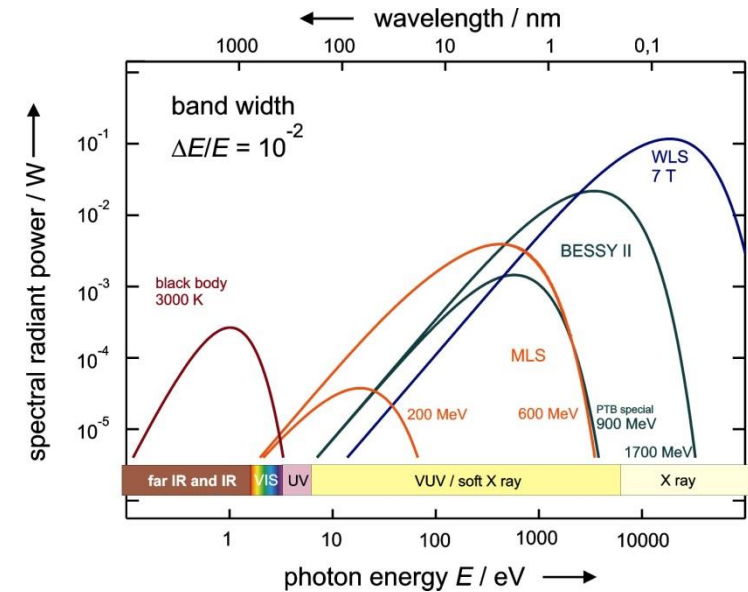
PTB laboratory at BESSY II: well-known synchrotron radiation for x-ray radiometry and x-ray spectrometry



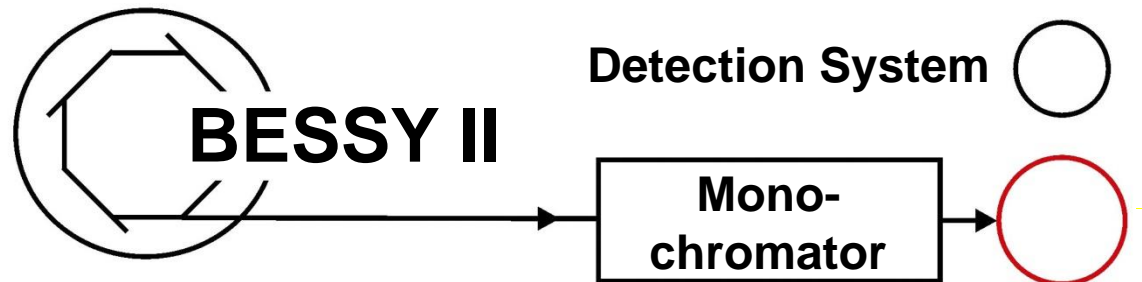
Source-based Radiometry:



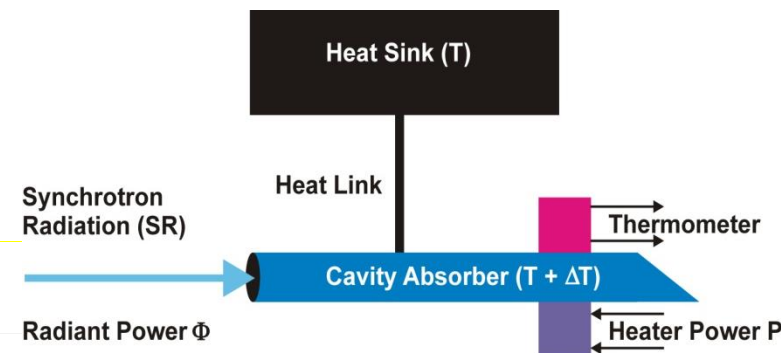
Primary Source Standard
 (Relative Standard Uncertainty: $u = 0.1 \%$)



Detector-based Radiometry:



Primary Detector Standard
 (Cryogenic Radiometer, Relative Standard
 Uncertainty: $u = 0.1 \%$)

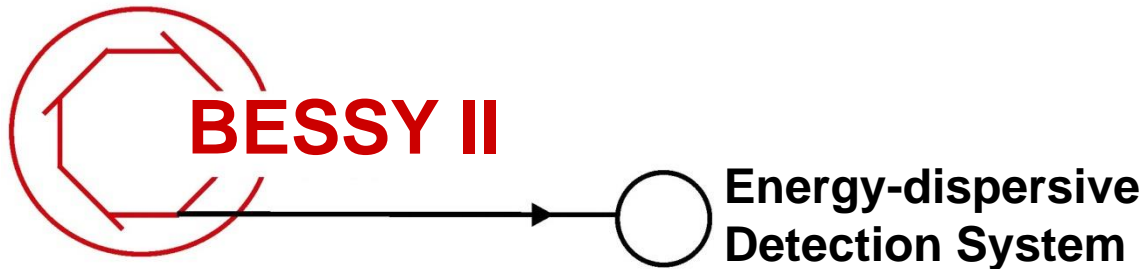


For constant absorber temperature $T + \Delta T$:

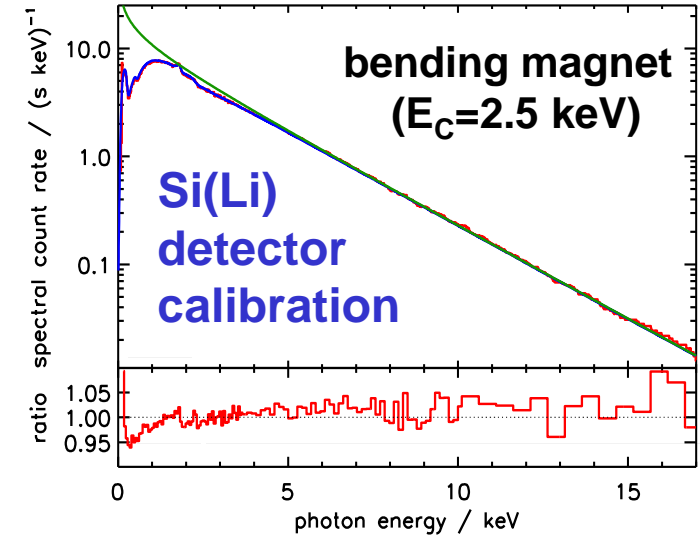
$$\Phi = P_{SR\ off} - P_{SR\ on} \quad (\text{Electrical Substitution})$$

PTB laboratory at BESSY II: well-known synchrotron radiation for the calibration of x-ray instrumentation

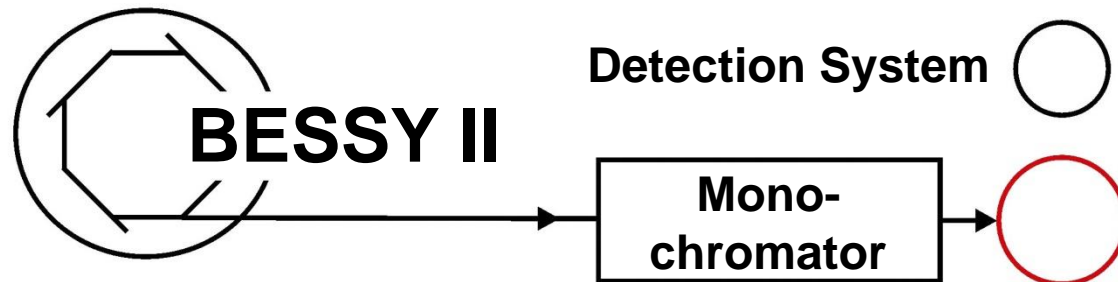
Source-based Radiometry:



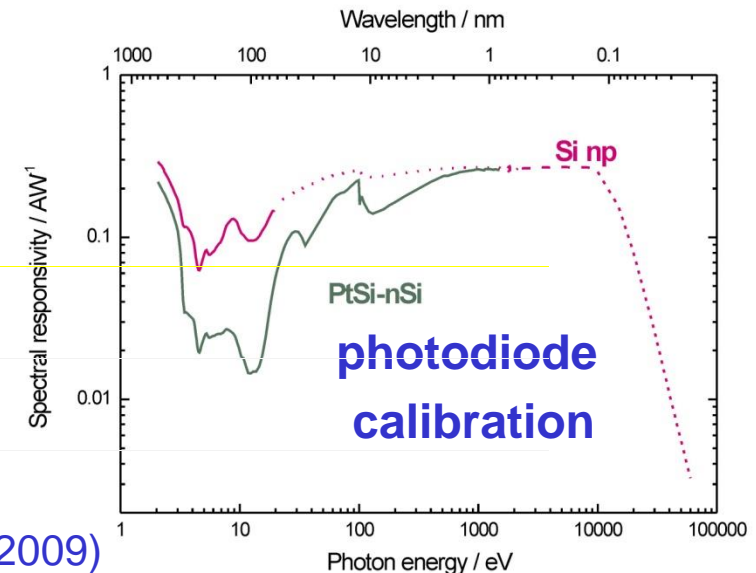
Primary Source Standard
(Relative Standard Uncertainty: $u = 0.1 \%$)



Detector-based Radiometry:



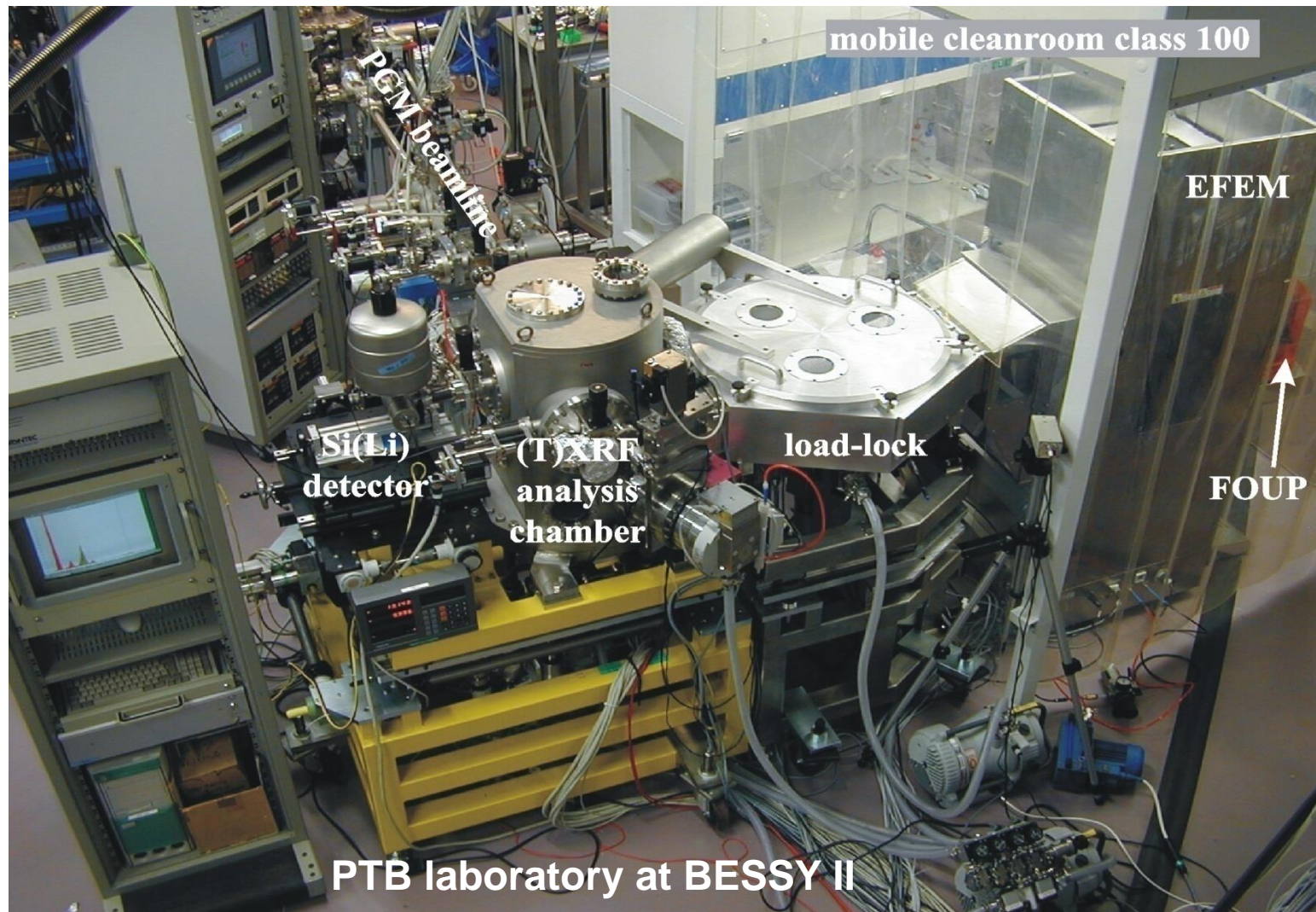
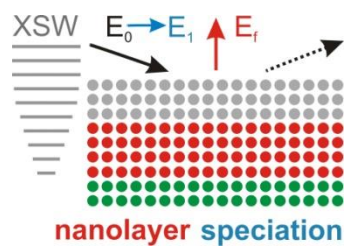
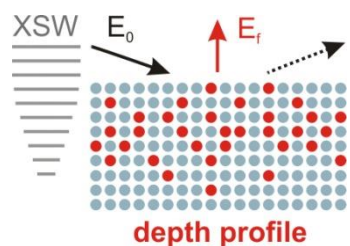
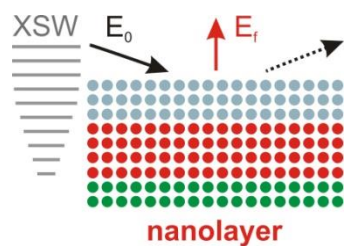
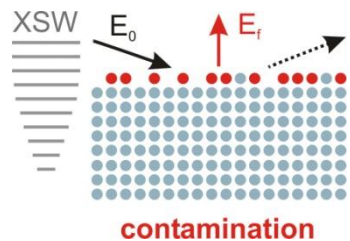
Primary Detector Standard
(Cryogenic Radiometer, Relative Standard
Uncertainty: $u = 0.1 \%$)



Total-reflection X-Ray Fluorescence (TXRF) facility for 200 and 300 mm Si wafers using synchrotron radiation



X-ray and IR spectrometry



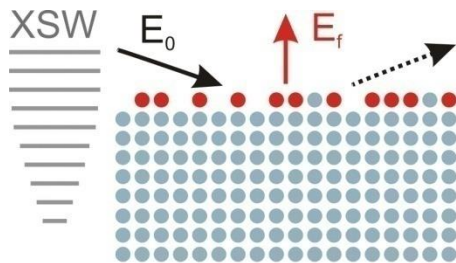
PTB laboratory at BESSY II

reference based TXRF - Ni surface contamination

Total-reflection X-ray Fluorescence (TXRF) analysis:

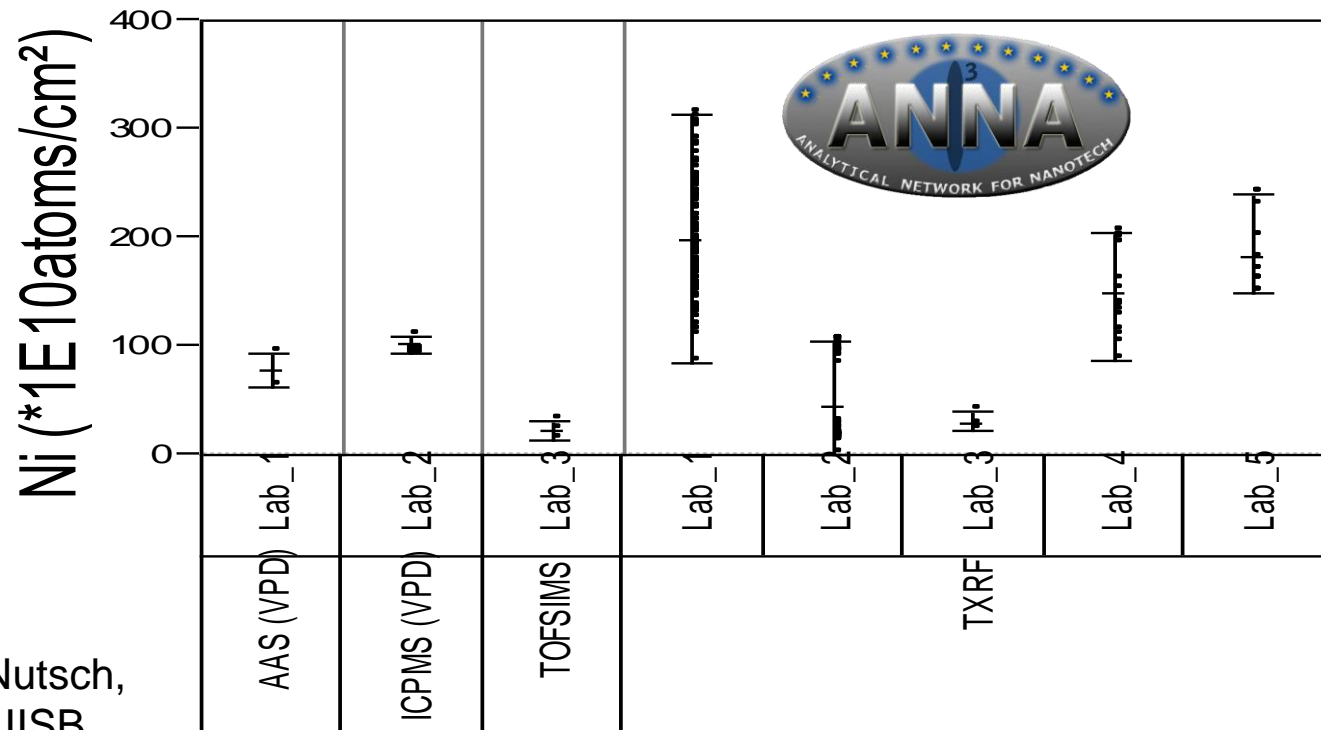
- non-consistent results from round robin tests (differences up to a factor of ten)
- reason: problems with employed calibration samples (droplet depositions)

spin coated contamination:
 metals 1×10^{12} atoms/cm²
 and light elements (Na, Al)
 1×10^{13} atoms/cm²

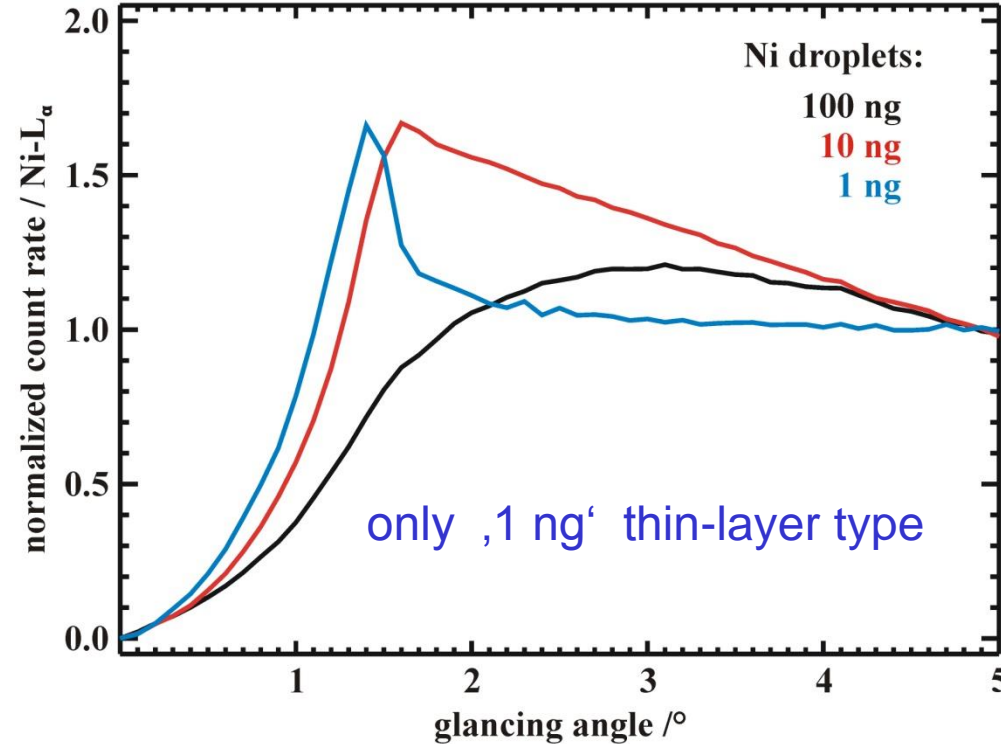
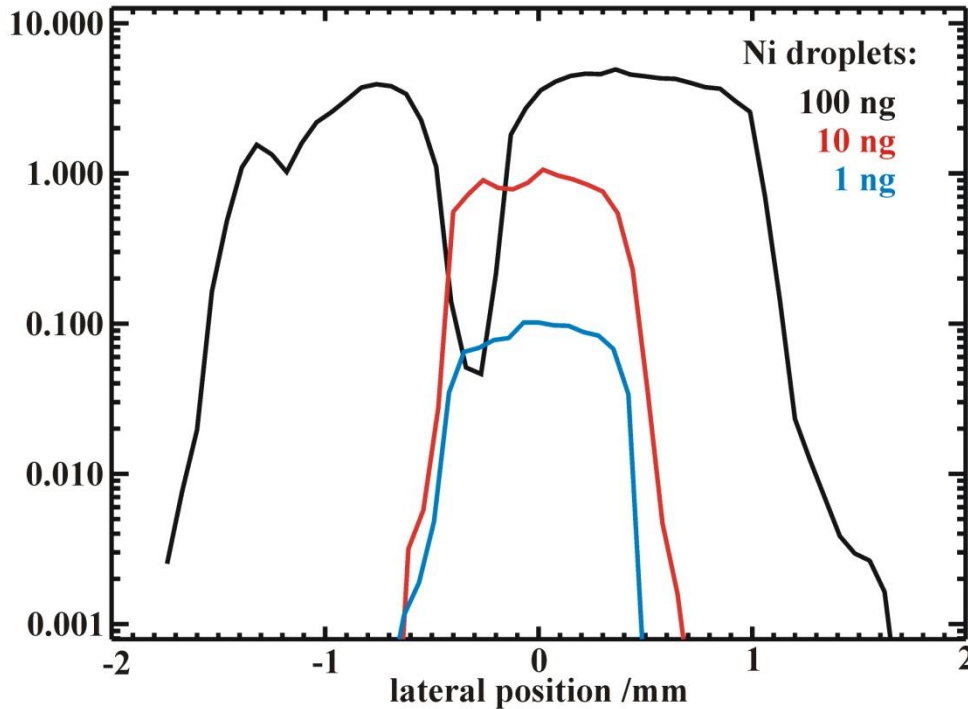


contamination

A. Nutsch,
 FhG IISB



Assessment of TXRF calibration samples for Ni surface contamination



Reason for deviations in contamination results: inhomogeneities and absorption saturation of TXRF calibration droplets
→ “slicing” and “angular scanning” of calibration droplets by reference-free TXRF as validation technique

